

Characterization and Preservation Techniques of Plant Xylem as Low Cost
Membrane Filtration Devices

By

Benjamin R. Potash

Submitted to the
Department of Mechanical Engineering
In Partial Fulfillment of the Requirements for the Degree of

Bachelor of Science in Mechanical Engineering

at the

Massachusetts Institute of Technology

June 2014

© 2014 Massachusetts Institute of Technology. All rights reserved.

Signature of Author: _____
Department of Mechanical Engineering
May 9, 2014

Certified by: _____
Rohit Karnik
Associate Professor of Mechanical Engineering
Thesis Supervisor

Accepted by: _____
Annette Hosoi
Professor of Mechanical Engineering
Undergraduate Officer

This Page Intentionally Left Blank

Characterization and Preservation Techniques of Plant Xylem as Low Cost Membrane Filtration Devices

By

Benjamin R. Potash

Submitted to the
Department of Mechanical Engineering
In Partial Fulfillment of the Requirements for the Degree of
Bachelor of Science in Mechanical Engineering

Safe drinking water remains inaccessible for roughly 1.1 billion people in the world.³⁴ As a result, 400 children under the age of 5 die every hour from biological contamination of drinking water.³⁴ Studies have been done to show that plant xylem from the sapwood of coniferous trees is capable of rejecting 99.99% of bacteria from feed solutions.¹⁶ Additionally, 4 L/d of water can be filtered with a $\sim 1 \text{ cm}^2$ filter area using a transmembrane pressure of 5 psi, an amount sufficient to meet the drinking needs of one person. However, the main drawback of xylem is that its permeability drops by a factor of 100 or more after being left out to dry for only a few hours. This paper seeks to characterize the performance of the xylem as a filter, determine the minimum length at which the xylem is effective for filtering bacteria, and increase the xylem's ability to rewet (retaining its permeability and rejective capabilities) after drying through the use of polymer coatings. Finally, potential techniques for decreasing the minimum particulate size the xylem can filter are discussed, with the aim of allowing the membrane to filter viruses.

Thesis Supervisor: Rohit Karnik

Title: Associate Professor of Mechanical Engineering

This Page Intentionally Left Blank

Acknowledgements

I cannot thank my thesis supervisor, Professor Rohit Karnik, enough for everything he's done for me. Without his continued support and guidance throughout this project, none of this would have been possible. I'd also like to thank my undergraduate academic advisor, Professor Sang-Gook Kim, who put me in touch with Prof. Karnik and helped me find this project in the first place.

A big thank you to the other members of my lab who worked on this project before me and continued the research with me, Michael Boutilier, Jongho Lee, & Valerie Chambers. They were always ready to offer help whenever I needed it.

I'd also like to acknowledge the support of the MIT Facilities Department, specifically Daniel Caterino & Todd Gillan, who helped me gather the samples for testing and were always there when I needed a fresh supply.

This Page Intentionally Left Blank

Table of Contents

1.	Introduction	11
1.1.	The Need for Low Cost Filters	11
1.2.	Current Solutions	12
1.3.	Membrane Filtration	12
2.	Background	15
2.1.	Previous Work	15
2.2.	Plant Xylem Structure	15
3.	Sample Preparation	19
3.1.	Gathering Samples	19
3.2.	Storage Between Tests & Freshness	20
3.3.	General Sample Preparation & Setup	20
4.	Directional Dependence	24
4.1.	Purpose of Experiment	24
4.2.	Test Specific Experimental Setup & Preparation	24
4.3.	Permeability Measurements	24
4.4.	Rejection Rate Measurements	26
4.5.	Conclusion	29
5.	Rejection Rate vs. Sample Length	30
5.1.	Purpose of Experiment	30
5.2.	Red Dye & Xylem Sample Preparations	30
5.3.	Red Dye Rejection Rates	30
5.4.	Fluorescent Particle Sample Preparation	36
5.5.	Fluorescent Particle Rejection Rates	37
5.6.	Conclusion	38
6.	Charles River Water Filtration	39
6.1.	Purpose of Experiment	39
6.2.	Gathering Sample & Preparation	39
6.3.	Filtration Results	39
6.4.	Conclusion	41
7.	Filtration Fouling Testing	42
7.1.	Purpose of Experiment	42
7.2.	Sample Preparation	42
7.3.	Fouling Results	43
7.4.	Conclusion	46
8.	Preservation Techniques	47

8.1.	Purpose of Experiment	47
8.2.	Background & Theory	47
8.3.	Polymer Research, Selection, & Solution Preparation	47
8.4.	Testing Procedure	49
8.5.	Effect of Coating on Permeability after Drying	51
8.6.	Effect of Coating on Rejection Rate	54
8.7.	Conclusion	55
9.	Conclusion.....	56
10.	Future Work	58
10.1.	Other Species	58
10.2.	Alternative Setups	59
10.3.	Other Coatings and Coating Techniques	59
10.4.	Virus Filtration.....	60
10.5.	Preparation & Packaging	60
10.6.	Removing Fouled Portion	61
10.7.	Implementation	61
	Bibliography	62
	Appendix A: Additional References on Filtration	65
	Appendix B: Uncertainty Analysis Resources.....	66

List of Figures

Figure 1-1 Dead-End and Cross Flow Filtration.....	12
Figure 1-2 Different Filtration Methods	13
Figure 2-1 Xylem Structure	17
Figure 3-1 Eastern White Pines (Pinus Strobus).....	19
Figure 3-2 Branch Storage	20
Figure 3-3 Portion of Branch to be Removed.....	21
Figure 3-4 Various Methods for Cutting Samples.....	21
Figure 3-5 Steps Required to Prepare Xylem Filter.....	22
Figure 3-6 Nitrogen Tank Setup	23
Figure 4-1 Dependence of Permeability on Orientation.....	25
Figure 4-2 UV-Vis Probe.....	26
Figure 4-3 UV-Vis Absorption Data for Orientation Dependency Tests	27
Figure 4-4 Malvern Zetasizer Nano ZS	28
Figure 4-5 Particle size Distribution for Orientation Dependency Tests.....	29
Figure 5-1 Filtrates of Different Xylem Lengths for 1000x Dilution.....	31
Figure 5-2 Absorption Levels from 1000x Diluted Red Ink Calibration.....	32
Figure 5-3 Absorption Levels of Filtrates from 1000x Diluted Red Ink	32
Figure 5-4 Filtrates of Different Xylem Lengths for 300x Dilution.....	33
Figure 5-5 Cross Section View of Xylem Showing Ink Penetration	34
Figure 5-6 Absorption Levels from 300x Diluted Red Ink Calibration.....	34
Figure 5-7 Absorption Levels of Filtrates from 300x Diluted Red Ink	35
Figure 5-8 1 μ m Fluorescent Microspheres	36
Figure 5-9 Nikon TE2000-U Inverted Epifluorescence Microscope Setup.....	37
Figure 5-10 Fluorescent Microsphere Concentrations.....	38
Figure 6-1 Comparison of Unfiltered and Filtered Charles River	40
Figure 6-2 Absorption Curves for Charles River Water	40
Figure 6-3 Charles River Water observed on a C-Chip.....	41
Figure 7-1 Flow Rate Decline with Wumulative Volume Filtered.....	43
Figure 7-2 Normalized Decline in Flow Rate.....	44
Figure 8-1 Containers of Glycerol & PVP.....	48
Figure 8-2 Mettler Toldo AL104 Scale	49
Figure 8-3 Modified Experimental Setup with Hose Clamp.	50
Figure 8-4 Intial Coating Performance at Re-Wetting.....	51
Figure 8-5 Base of a Coated Xylem During Re-Wetting.....	52
Figure 8-6 Final Coating Performance at Re-Wetting.....	53
Figure 8-7 Ink Filtered using Re-WetCoated Xylem.....	54
Figure 8-8 Particle Size Distribution of the Permeates.....	55
Figure 10-1 Map Showing Indigenous Regions of Eastern White Pine	58
Figure 10-2 Diagram of a Traditional Membrane Bioreactor (MBR)	59
Figure 10-1 Flow Chart Used for Determining the Optimal Filtration Method	65

List of Tables

Table 1 – Summary Water Supply Diseases.....	11
Table 2 – Absorption Values for Oreintation Dependence.....	27
Table 3 – Absorption Values for Varying Lengths with 1000x Diluted Ink	33
Table 4 – Absorption Values for Varying Lengths with 300x Diluted Ink	35
Table 5 – Fouling Mechanisms and Governing Equations.....	45
Table 6 – Summary PVP Polymers	48
Table 7 – Summary of PVP Solutions	49
Table 8 – T-Factor Table Used for Uncertainty Analysis.....	66

1. Introduction

1.1. The Need for Low Cost Filters

Potable or drinking water is defined as having acceptable quality in terms of its physical, chemical, and bacteriological parameters so that it can be safely used for drinking and cooking.¹⁰ Safe drinking water remains inaccessible for about 1.1 billion people in the world.³⁴ As a result, 400 children under the age of 5 die every hour from biological contamination of drinking water.³⁴ The WHO estimate of the toll is more than 5 million deaths annually from unsafe drinking water.³⁴ WHO states that the “infectious diseases caused by pathogenic bacteria, viruses and protozoa or by parasites are the most common and widespread health risk associated with drinking water.”¹⁰ At any given time, about half the population in the developing world is suffering from one or more of the six main diseases associated with water supply and sanitation, summarized in Table 1 – Summary of the 6 main diseases associated with water supply and sanitation.¹⁰ The generally accepted value for the daily per capita consumption of water for a person weighing 60 kg is 2 liters,²⁹ while the maximum expected value is 8 liters for drinking and cooking.⁸

Table 1 – Summary of the 6 main diseases associated with water supply and sanitation

Disease	People Affected	Major Health Concerns	Minimum Size
1). Diarrhea	1.7 billion cases per year ³¹	Inhibits body’s ability to absorb nutrients, dehydration, stunted growth from malnutrition, ¹⁰ kills 760,000 children under five annually ³¹	Substantial Variation (viral and bacterial)
2). <i>Ascaris</i>	> 1.4 billion (25% of population) ²⁵	Intestinal blockage and impaired growth in children ⁴	45-70 x 35-50 μm . ²⁵
3). <i>Dracunculiasis</i>	< 1800 new cases reported annually ³⁰	Oedema, a blister and eventually an ulcer, accompanied by fever, nausea, and vomiting ³⁰	490-737 x 18-24 μm ²²
4). Hookworm	576 million ⁹	Rarely fatal but infected people become non-functional for months (crippling pain) ³²	64-76 x 35-40 μm ¹⁵
5). <i>Schistosomiasis</i>	210 million ⁹	Up to 200,000 people die from it a year ²⁶	140 x 60 μm ²⁸
6). Trachoma	84 million active cases ³³	8 million people irreversibly visually impaired, approximately 3% of world’s blindness ³³	0.3 μm in diameter ⁵

1.2. Current Solutions¹⁶

Current solutions exist for today for disinfecting and purifying water, including: chlorination, filtration, UV-disinfection, pasteurization or boiling, and ozone treatment.¹⁰ While each of these has its own strengths in certain area, all of them have significant drawbacks that make them non-ideal for personal use in developing countries. Chlorine treatment is effective on a large scale, but would be too expensive for smaller towns and villages. While this strategy would be most cost effective for controlling microbial growth at the water source, controlling water quality at the point-of-use is often more effective due to the issues of microbial regrowth, byproducts of disinfectants, pipeline corrosion, and contamination in the distribution system.¹⁸ Boiling is an effective method to disinfect water; however, the amount of fuel required to disinfect water by boiling is several times more than what a typical family will use for cooking.¹⁰ UV-disinfection is the most promising point-of-use technology available;¹⁰ however, this process requires access to electricity and has the additional cost and labor requirement maintaining the UV lamp. While small and inexpensive filtration devices can potentially address the issue of point-of-use disinfection, an ideal technology does not currently exist. Inexpensive household carbon-based filters are not capable of removing pathogens and can be used only when the water is already biologically safe.¹⁰ Sand filters that can remove pathogens require large area and knowledge of how to maintain them,¹⁰ while membrane filters capable of removing pathogens¹⁸ suffer from high costs, fouling, and require pumping power due to low flow¹⁷ rates that prevents their wide implementation in developing countries. In this context, new approaches that can improve upon current technologies are urgently needed. Specifically, membrane materials that are inexpensive, readily available, disposable, and effective at pathogen removal could greatly impact our ability to provide safe drinking water to the global population.¹⁶

1.3. Membrane Filtration

Membrane filtration works through the use of a semi-permeable media with special pore sizes that prevent particles larger than the pores from passing through them. Membrane filtration can be set in one of two different configuration: dead-end filtration, or cross-flow filtration (shown below).

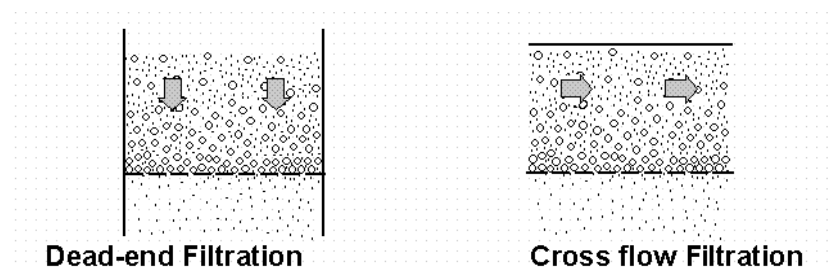


Figure 1-1 Diagram depicting the difference between dead-end and cross flow filtration²¹

This can be used to cheaply and effectively separate a solution of dissolved particles from their solvent. The potential to drive flow across the membrane can either come from concentration gradients or transmembrane pressure. The capital cost of MF systems on a basis of dollars per volume of installed treatment capacity, does not escalate rapidly as plant size decreases. This factor makes membranes quite attractive for small systems, such as those intended for personal use.¹⁹ When selecting which media one should use for filtering a solution, it is best to directly consider the pore size by looking at the molecular weight cutoff (MWCO) and the applied pressure needed to run the membrane system.¹⁹ There is a large range of particles sizes that membrane filtration can successfully reject. They can be divided up into several regimes: particle filtration, microfiltration, ultrafiltration, and nanofiltration, where the effective length scales for the particles in each regime are shown below.

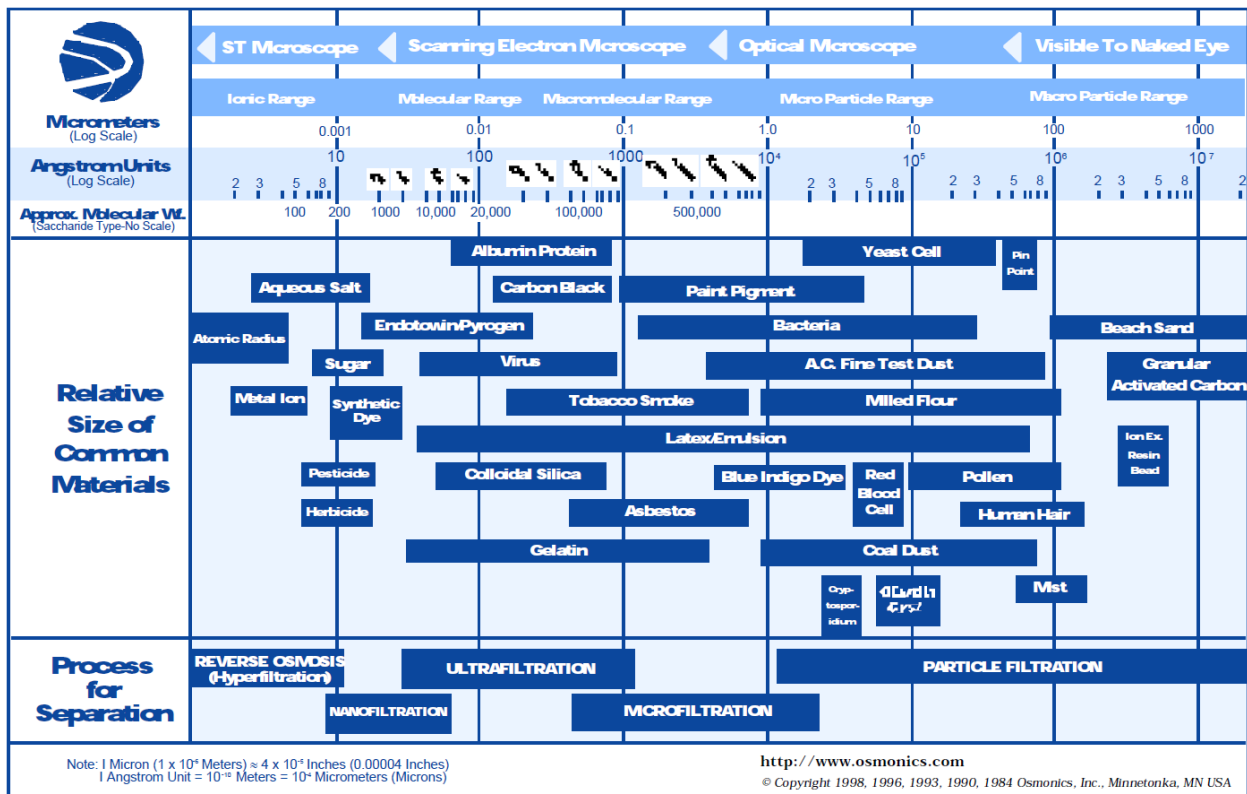


Figure 1-2 Chart showing the regimes different filtration methods operate in as well as common particles which are that size

Microfiltration (MF) has significant applications in simple dead-end filtration of particles 0.03 to 10 microns¹⁹ because it can operate at relatively low pressures.¹ MF is not an absolute barrier to viruses; however, when used in combination with disinfection, MF appears to control microorganism growth in water.¹⁹ It is recommended that prefilters be used to remove large particles that may plug the inlet to the fibers within the membrane module.¹⁹ Ultrafiltration is generally used to remove particles that are 0.002 to 0.1 microns, which includes all bacteria and

some, but not all, viruses.¹ Finally nanofiltration, is generally targeted to only remove divalent and larger ions,¹ with approximate nominal pore sizes of 0.001 microns.¹⁹ As a comparison, an average household coffee filter has a lower bound of 10 to 15 microns. And the smallest particle the naked human eye can detect is roughly 1 micron.²²

2. Background

2.1. Previous Work

This thesis builds upon the work done by Jongho Lee, Michael S. H. Boutillier, Valerie Chia, and Professor Rohit Karnik at the Massachusetts Institute of Technology in Cambridge, MA. The paper they published, “Water Filtration Using Plant Xylem” served as both the inspiration and framework around which the following experiments were designed. This thesis uses the same basic experimental setup and many of the same test procedures, such as using diluted red dye-pigment ink as a feed solution to measure rejection rates. However, I seek to answer different questions and characterize different features of the xylem as a potential filter.

In their paper, the researchers determined that the fresh cut xylem had a permeability on the order of $\sim 5\text{-}6 \times 10^{-10}$ m²/Pa-s and was able to successfully reject >99.99% of fluorescently labeled *Escherichia coli* bacteria.¹⁶ This meant that roughly a $\sim 1\text{cm}^2$ sample could successfully serve as a filter for bacteria with a flow rate of $\sim 4\text{L/d}$ under 5 psi of pressure (or 0.7-3.5 m of gravitational pressure head), which is enough to meet the drinking water requirements of one person.¹⁶ Using the red ink, they were able to determine the minimum particle cutoff length to be 100 nm.¹⁶

They also identified and discussed some of the major challenges that needed to be addressed before the xylem could be implemented as low-cost water filter for developing countries. The first primary concern was that, after drying, the xylem would either lose its permeability, suggesting that the membranes became clogged, or retain their permeability but lose their ability to reject particles, suggesting the membranes tore or were damaged.¹⁶ This also held true for commercially available kiln-dried wood.¹⁶ The second major concern is that the xylem was unable to filter viruses. The cutoff length for the xylem was roughly 100 nm, while viruses have a length scale of around 20 to 100 nm.¹⁶ For my work, I chose to address these concerns as well as others.

2.2. Plant Xylem Structure¹⁶

The following is taken directly from *Water Filtration Using Plant Xylem* by Jongho Lee & Michael H.S. Boutillier. It is reproduced here for convenience.

The flow of sap in plants is driven primarily by transpiration from the leaves to the atmosphere, which creates negative pressure in the xylem. Therefore, xylem evolution has

occurred under competing pressures of providing minimal resistance to the flow of sap, while protecting against cavitation (i.e. nucleation) and growth of bubbles that could stop the flow of sap and kill the plant, and to do this while maintaining mechanical strength.²⁴ The xylem structure comprises many small conduits that work in parallel and operate in a manner that is robust to cavitation,²⁴ (Figure 2-1). In woody plants, the xylem tissue is called the sapwood, which often surrounds the heartwood (i.e. inactive, non-conducting lignified tissue found in older branches and trunks) and is in turn surrounded by the bark (Figure 2-1b,c). The xylem conduits in gymnosperms (conifers) are formed from single dead cells and are called tracheids (Figure 2-1c), with the largest tracheids reaching diameters up to 80 μm and lengths up to 10 mm.²⁴ Angiosperms (flowering plants) have xylem conduits called vessels that are derived from several cells in a single file, having diameters up to 0.5 mm and lengths ranging from a few millimeters to several meters.²⁴ These parallel conduits have closed ends and are connected to adjacent conduits via “pits”⁷ (Figure 2-1d,e). The pits have membranes with nanoscale pores that perform the critical function of preventing bubbles from crossing over from one conduit to another. Pits occur in a variety of configurations; Figure 2-1d,e show torus-margo pit membranes that are shaped like a donut (margo) with an impermeable part in the center called torus, occurring in conifers.^{7, 14} More interestingly, the porosity of the pit membranes ranges in size from a few nanometers to a few hundred nanometers, with pore sizes in the case of angiosperms tending to be smaller than those in gymnosperms.⁷ Pit membrane pore sizes have been estimated by examining whether gold colloids or particles of different sizes can flow through.^{6, 7} Remarkably, it was observed that 20 nm gold colloids could not pass through inter-vessel pit membranes of some deciduous tree species,⁶ indicating an adequate size rejection to remove viruses from water. Furthermore, inter-tracheid pit membranes were found to exclude particles in the 200 nm range,⁷ as required for removal of bacteria and protozoa.

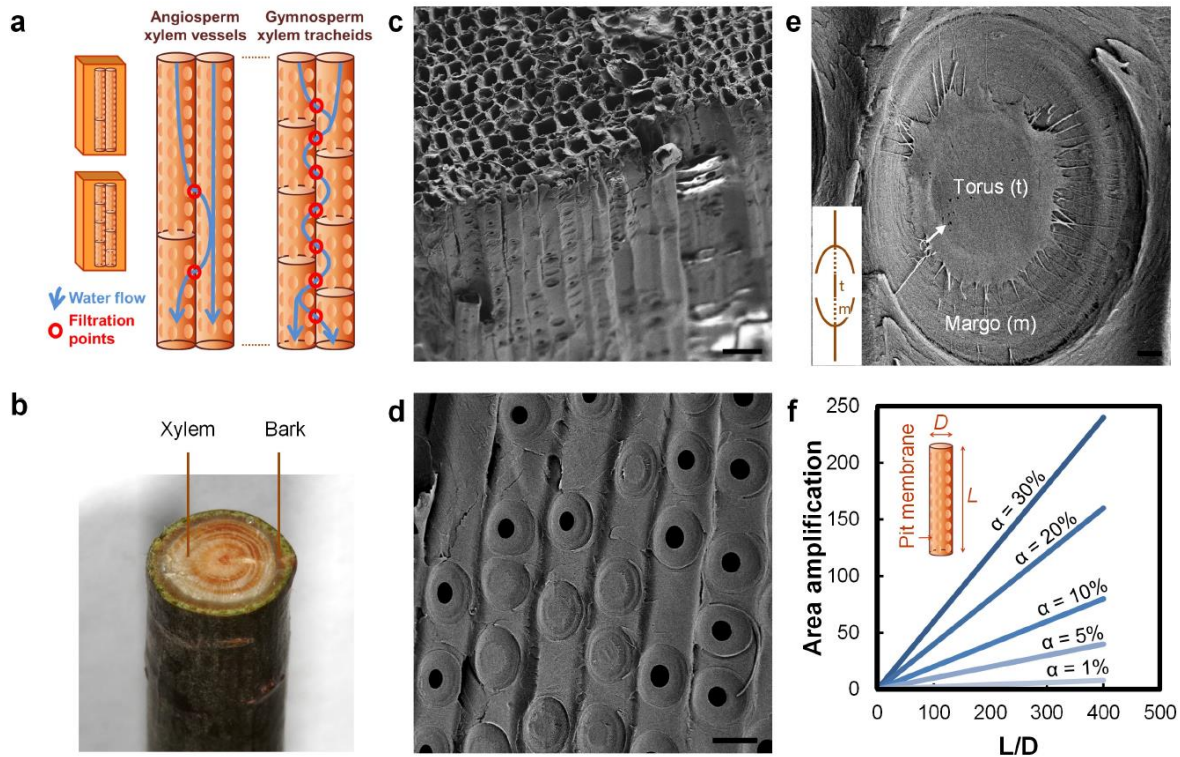


Figure 2-1 Xylem structure. a) Structure of xylem vessels in flowering plants and tracheids in conifers. Longer length of the vessels can provide pathways that can bypass filtration through pit membranes that decorate their circumference. b) Photograph of ~ 1 cm diameter pine (*pinus strobus*) branch used in the present study. c) Scanning electron microscope (SEM) image of cut section showing tracheid cross section and lengthwise profile. Scale bar is 40 μm . d) SEM image showing pits and pit membranes. Scale bar is 20 μm . e) Pit membrane with inset showing a cartoon of the pit cross-section. The pit cover has been sliced away to reveal the permeable margo surrounding the impermeable torus. Arrow indicates observed hole-like structures that may be defects. The margo comprises radial spoke-like structures that suspend the torus that are only barely visible overlaying the cell wall in the background. Scale bar 1 μm . f) Dependence of the area amplification, defined as the pit membrane area divided by the nominal filter area, on the tracheid aspect ratio L/D and fractional area α occupied by pit membranes.

Since angiosperms (flowering plants, including hardwood trees) have larger xylem vessels that are more effective at conducting sap, xylem tissue constitutes a smaller fraction of the cross-section area of their trunks or branches, which is not ideal in the context of filtration. The long length of their xylem vessels also implies that a large thickness (centimeters to meters) of xylem tissue will be required to achieve any filtration effect at all – filters that are thinner than the average vessel length will just allow water to flow through the vessels without filtering it through pit membranes (Figure 2-1a). In contrast, gymnosperms (conifers, including softwood trees) have short tracheids that would force water to flow through pit membranes even for small thicknesses (< 1 cm) of xylem tissue (Figure 2-1a). Since tracheids have smaller diameters and are shorter, they offer higher resistance to flow, but typically a greater fraction of the stem cross-section area

is devoted to conducting xylem tissue. For example, in the pine branch shown in Figure 2-1b used in this study, fluid-conducting xylem constitutes the majority of the cross-section. This reasoning leads us to the conclusion that in general the xylem tissue of coniferous trees – i.e. the sapwood is likely to be the most suitable xylem tissue for construction of a water filtration device, at least for filtration of bacteria, protozoa, and other pathogens on the micron or larger scale.

The resistance to fluid flow is an important consideration for filtration. Pits can contribute a significant fraction (as much as 30-80%)^{7, 24} of the resistance to sap flow, but this is remarkably small considering that pit membrane pore sizes are several orders of magnitude smaller than the tracheid or vessel diameter. The pits and pit membranes form a hierarchical structure where the thin, highly-permeable pit membranes are supported across the microscale pits that are arranged around the circumference of the tracheids (Figure 2-1a). This arrangement permits the pit membranes to be thin, offering low resistance to fluid flow. Furthermore, the parallel arrangement of tracheids with pits around their circumference provides a high packing density for the pit membranes. For a given tracheid with diameter D and length L , where pit membranes occupy a fraction α of the tracheid wall area, each tracheid effectively contributes a pit membrane area of $\pi DL\alpha/2$, where the factor of 2 arises as each membrane is shared by two tracheids. However, the nominal area of the tracheid is only $\pi D^2/4$, and therefore, the structure effectively amplifies the nominal filter area by a factor of $2\alpha(L/D)$ (Figure 2-1f). The images in Figure 2-1c indicate $D \sim 10-15 \mu\text{m}$, $\alpha \sim 0.2$, yielding an effective area amplification of ~ 20 for tracheid lengths of 1-2 mm. Therefore, for a filter made by cutting a slice of thickness $\sim L$ of the xylem, the actual membrane area is greater by a large factor due to vertical packing of the pit membranes. Larger filter thicknesses further increase the total membrane area, but the additional area of the membrane is positioned in series rather than in parallel and therefore decreases the flow rate, but potentially improves the rejection performance of the filter.

3. Sample Preparation

3.1. Gathering Samples

White pine samples, also known as *pinus strobus*, were used for all of the experiments performed throughout this document. These samples were harvested from various locations across the campus of the Massachusetts Institute of Technology, located in Massachusetts, USA. Early stage tests were done using younger trees that were freshly planted outside the McCormick dormitory; however, the tests published in this paper were validated using older trees located in Cambridge, MA. It is unclear at the moment what effects, if any, the age of the tree may have on the performance and viability of the samples as filters. Branches roughly 0.5-1.0" in diameter were trimmed from the tree using pruning shears and immediately placed in a bucket of water to prevent drying out while there were being transported to the lab.



Figure 3-1 One of the Eastern White Pines (*pinus strobus*) that was used to collect samples

3.2. Storage Between Tests & Freshness

All branches were stored together in the same bucket full of water. It is recommended that the water be changed at least every other day to keep the xylem fresh longer. Under these conditions, some xylem still allowed flow to permeate the membrane while rejecting particles roughly a month after it had been cut from the tree. However, there was significant variation in this window, as other samples lasted only two weeks.



Figure 3-2 The branches being stored together in a bucket of water in the lab between tests

3.3. General Sample Preparation & Setup

The following is the general procedure followed for the majority of the tests carried out. Consult the lab specific setup for each test for notes on anything that deviated from this process. To prepare a sample for an experiment, a branch was selected from the bucket that fit the specific criteria for that test. Within a single experimental run, multiple xylem samples were needed with uniform filtration performance, that way any changes in the results were a direct effect of the single

operating parameter that was changed. Therefore, the most ideal branches had long straight sections with uniform cross-sectional area. We also wanted to select a branch that had a diameter larger than the inner diameter of our rubber tubing, so once the bark was removed, the sample would still press fit snugly into the tubing.

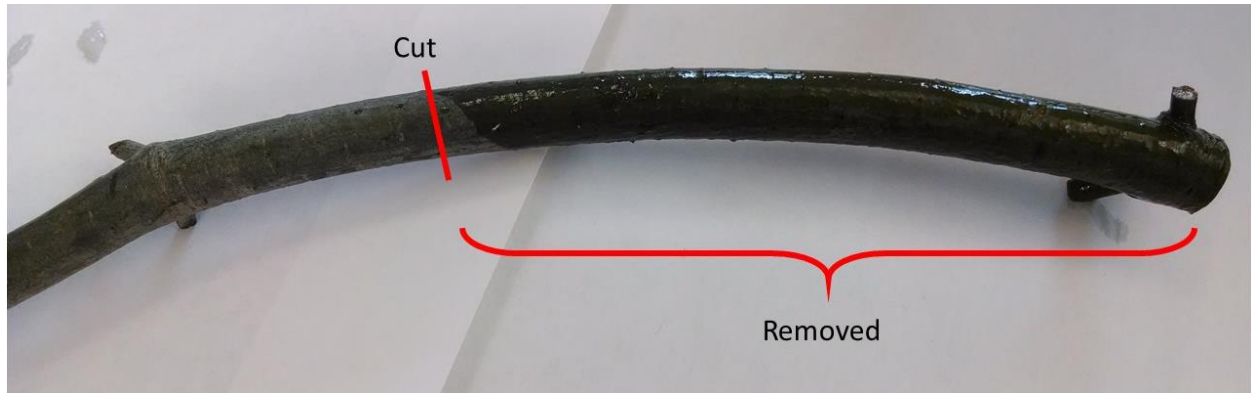


Figure 3-3 Diagram showing the portion of the branch that needs to be removed before testing due to water damage

After the sample was removed, the lower portion that had been submerged in the water during storage was removed, it is unclear at the moment how the xylem is effected by being submerged under water. However, this isn't representative of the nominal conditions in nature, so we started at the portion where the bark was exposed to the air. The branch was marked with a sharpie by placing a dot at the center to later be used for orienting the branch in the experimental rig. The center was chosen because experiments have shown that the pith and heartwood of the branch aren't responsible for filtration. The branch was measured to the desired length and cut using single edge industrial razor blade. A Kwik Cut hose and pipe cutter was also used as a potential means of cutting the samples; however, testing revealed that this trimmer cracked the samples down the center, rendering them unusable as filters. The standard length used for testing was roughly 0.5in.



Figure 3-4 (Middle) Two samples cut with (Left) Kwik Cut pipe cutter and (Right) industrial razors, the left sample has a crack through the center of it, compromising it's capability as a filter

The bark was then peel from the samples by hand. This was a way to tell whether the samples were still fresh or not, if they were than the bark would peeled off cleanly in one continuous piece. If the branch dried out, they needed to be cut off with a razor or peeled in pieces.

For these tests, we used flexible rubber hosing with an inner diameter of 3/8in, so many times the samples needed to be trimmed down to fit snugly inside the tubing. In previous work, five minute cure epoxy was used to seal around the xylem sample; however, we used larger branches that press fit into the hosing, and stretched it out to form an airtight seal, preventing leakage during the tests and eliminating the need for epoxy for most tests. The sample was then clamped in place by tightening down a hose clamp around the top portion of the xylem. Additionally, the end of the tube was sealed using a stretchable parafilm as an added precaution.



Figure 3-5 The steps required to prepare a xylem sample for filtering¹⁶

In order to eliminate any variation in permeability or rejection rate due to the orientation of the branch, all samples were marked with a dot on the same side (the side of the branch that would have been facing the base of the tree). The default orientation was having the dot side loaded into the tube, so that water would flow through the branch in the same direction as in nature when it is carried up through the xylem from the roots to the leaves.

The flexible hose was then held in a vertical configuration with a ring stand. A 20ml disposable glass scintillation vial was placed underneath the hosing to collect the filtrate. Initially, the samples were full of sap, which needed to be removed before testing could occur; otherwise the sap could contaminate the filtrate. 10 ml of de-ionized water was loaded into the rubber hosing and it was connected to a pressurized nitrogen gas tank with an Airgas Single Stage Brass 0-100 psi Analytical Cylinder Regulator (CGA580). All tests were performed at 10 psi. In between tests, the rubber hose was flushed with water and organic solvents to remove any particulates from the previous run.



Figure 3-6 A picture of the compressed nitrogen tank and Airgas pressure regulator used to drive the flow

4. Directional Dependence

4.1. Purpose of Experiment

This was the first experiment that was run because if there was directional dependence, then there needed to be a method for keeping track of orientation; however, if there wasn't a significant difference in both of these aspects than that would eliminate the extra step of marking. Since water typically only flows in one direction through the xylem, the structure may have evolved to have a lower resistance to flow in that direction and a higher resistance in the opposite direction to prevent backflow. Additionally, the cross sections of the branches change as you move from the trunk to the needles so this physical asymmetry may lead to asymmetric properties.

4.2. Test Specific Experimental Setup & Preparation

The setup for this test followed the general preparation procedures in section 3.3 with the inclusion of a few additional steps. After the sample was flushed with 10 ml of de-ionized water, it was then removed from the hosing, flipped in orientation, and flushed again using the same process. This was to ensure sap had been cleared from the sample in both directions.

The rejection rate of the xylem was tested using a diluted solution of Higgins red pigment dye-based ink. The red ink was prepared by diluting 100 μl of red dye 1200x with de-ionized water. It was then thoroughly mixed and sonicated using a VWR symphony Ultrasonic Cleaner to break up any amalgamations of particles. The red ink contains a distribution of particle sizes varying from 70 to 500nm, which was determined using dynamic light scattering (DLS).¹⁶

4.3. Permeability Measurements

In order to determine whether the flow rate was dependent on orientation or not, two separate samples were prepared and tested independently. The first sample was initially loaded into the hosing in the standard orientation with the dot facing up. 10 ml of de-ionized water was loaded into the hose and then connected to the nitrogen gas. A butterfly valve at the connection to the tank was opened and the time it took to filter the 10 ml of water was recorded. Then the sample was removed, re-inserted in the opposite orientation, sealed again, and the time to filter 10 ml of water was recorded again. This process was repeated until 5 measurements were taken for each orientation. Then, to eliminate any bias from the sample initially being flushed in the standard

orientation, the second sample was initially flushed in the reverse orientation. Again, 5 measurements for each side were taken.

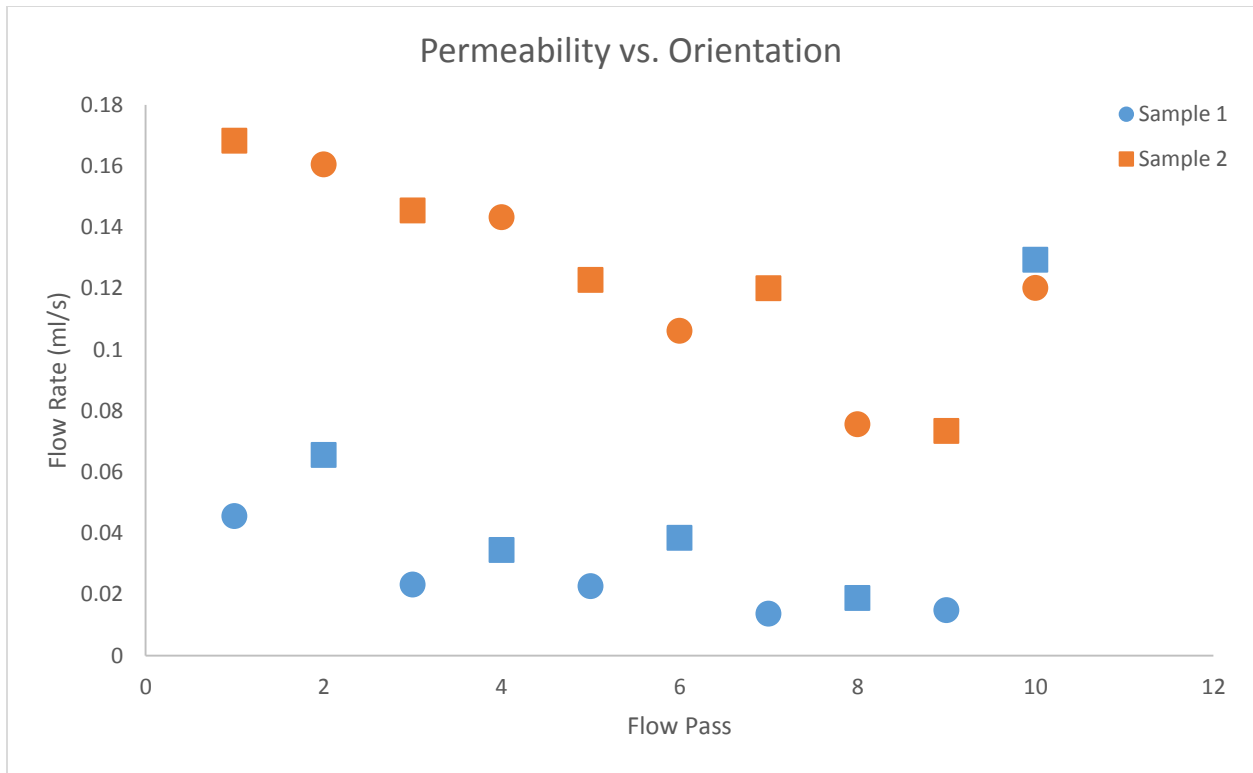


Figure 4-1 Graph depicting the dependence of permeability on orientation. Sample 1 was initially placed in the default orientation, while sample 2 was placed in the opposite orientation. Circles denote measurements taken in the standard orientation while squares denote measurements taken in the reverse orientation.

For the graph shown above, sample 1 was placed in the standard orientation for the first flush, while sample 2 was initially placed in the opposite orientation. Circles denote a measurement taken in the standard orientation, while squares refer to a measurement taken in the reverse orientation. The overall trend of the data is that the flow rate decreases as a higher cumulative volume of water is flushed through xylem. For the final measurements of sample 1 and Sample 2 this trend doesn't hold. Both of these values are the final of the 10 measurements taken with each sample. It is possible that after that much filtration, some of the "pits" ruptured and allowed water to pass through cleanly. The pits can contribute 30%-80% of the resistance to sap flow,^{7, 24} so if they were to rupture, the flow rate could increase dramatically. This hypothesis could be confirmed by running red ink through the xylem to test whether the samples were still rejecting particulates. However, this wasn't determined until after the samples had dried and could no longer be reliably tested for rejection rate.

From the data above, the flow rates for samples oriented in the "B" configuration were consistently higher than in configuration "A." However, this difference was only marginal. To quantify whether this difference was significant, a student t-test was performed on both samples.

Including all 10 measurements for each samples, sample 1 had a student t-test p-value of 0.178 and sample 2 had a p-value of 0.760 for flow rates in standard vs. reverse orientations. Typically, a value of 0.05 is used as the threshold for the measurements to have statistical significance. If we assume the previous hypothesis about the pits rupturing to be true and neglect the final values on each side, we get values of 0.026 and 0.155. This means that sample 1 could show that the flow rate does depend on direction, and that placing samples in the reverse orientation allows for higher permeability. Due to conflicting results from the samples, additional testing needs to be done before a reliable conclusion can be drawn.

4.4. Rejection Rate Measurements

For this test, 2 ml of the 1200x diluted red ink was flushed through the xylem in its standard orientation and collected in a 20 ml glass vial. Then, the xylem was removed, inserted in the reverse orientation, re-fixture in the hosing, and back flushed with 10 ml of de-ionized water to remove any loose particles from the surface. Another 2 ml of red ink was flown through the xylem and collected in a new vial. We would expect to second side to have a higher rejection rate than the first because the particles filtered from the first run built up on the surface into a “cake layer.” Literature has shown that cake layer formation in membrane filtration increases the resistance to flow and can increase rejection rates because the cake forms an additional barrier for the particles to pass through (see section 7.1 for more detail on fouling). To eliminate this bias, a second sample was tested using the same procedure; however, this one was tested in the reverse orientation first, and then flipped, back flushed in the standard orientation, and flown with 2 ml of red ink. Both samples were cut from the same branch to minimize variability among the xylem.



Figure 4-2 (Left) UV-Vis probe used to measure turbidity of filtrate (Right) cuvette sample holder for probe

The relative rejection rates were determined using an Agilent Technologies Cary 60 UV-Vis Probe (shown below). The device works by measuring the amount of light that gets absorbed by a liquid sample placed in a cuvette. For these tests, 50 μL of the dye solution was placed into a cuvette for scanning. The probe was set to scan between 200 nm and 800 nm. After the absorption was measured at each wavelength, a definitive peak of 573 nm was chosen as the point of comparison. The 4 filtrate absorption values were calculated by removing the reference from the measurements using the following equation:

$$Abs(x) = \frac{[Abs(573) - Abs(700)]_{measured}}{[Abs(573) - Abs(700)]_{water}} \quad (1)$$

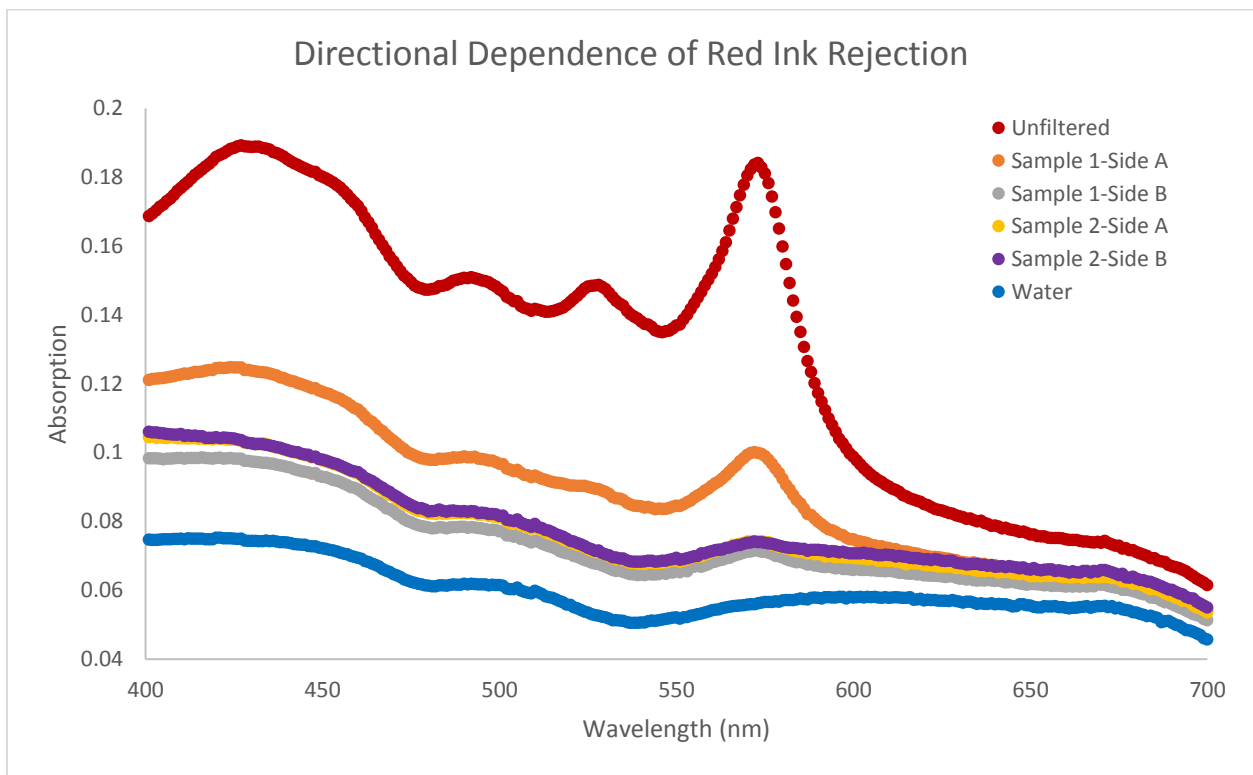


Figure 4-3 UV-Vis absorption data comparison showing rejection rate dependence on orientation

Table 2 – The absorption values for the various filtrates collected to test the dependence of rejection rate on orientation

Sample	Absorption Value	First or Second
Unfiltered	0.1121	N/A
Standard A	0.0352	First
Standard B	0.0097	Second
Reverse A	0.0101	Second
Reverse B	0.0084	First
Water	0.0000	N/A

From both the graph and table above, we can see that the first sample “standard” exhibited higher rejection of the ink particles during the 2nd pass when it was in the “B” orientation. This is to be expected since a “cake layer” of retentate formed on the surface during the first filtration, which increases the resistance of the membrane and allows it to remove smaller particles (see section 7.1 for an explanation of cake formation). For the second sample, we don’t observe this; instead, the two sides appear to exhibit identical rejection rates. However, during the second pass we would expect a higher rejection rate (assuming rejection doesn’t depend on orientation) due to the cake layer. This means that the xylem itself is worse at rejection in orientation “B” than in orientation “A” and that the two values are equal in this case because of the added rejection due to fouling from the ink particles.



Figure 4-4 Malvern Zetasizer Nano ZS used for dynamic light scattering (DLS) to determine particle sizes

Additionally, a Malvern Zetasizer Nano ZS was used to perform dynamic light scattering (DLS) on the samples to determine the particle size distribution for each permeate. Below is a graph showing the different distributions. It is unclear why all of the permeates maintained two peaks on the spectrum. For both the standard B and reverse A samples, this would be expected as some of the cake layer may have been forced loose into the collection vial as water passed through it. This could account for the larger chunks in the peaks centered around 300-500 nm. However, more interestingly, both samples shifted their peaks left when they were filtered for the second time. Namely, the Standard B had better rejection than Standard A, and Reverse A had better

rejection that Reverse B. This strongly supports the hypothesis that the cake layer improves rejection rate and decreases the cutoff particle size for the xylem. If this theory holds true, than fouling could be a method by which the xylem’s performance is tuned to allow it to filter viruses.

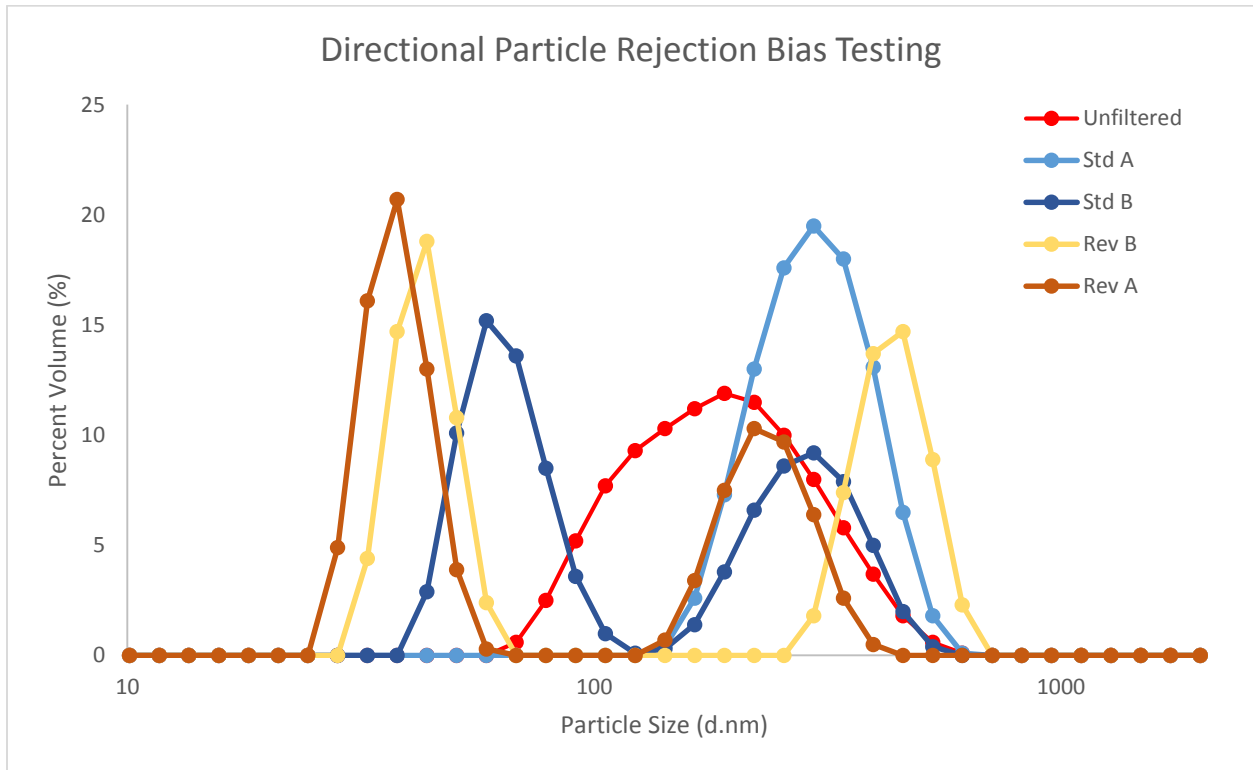


Figure 4-5 Graph showing the particle size distribution for the different feed solutions to compare directionality

4.5. Conclusion

The results from these tests suggest that the permeability of the xylem may depend weakly on the direction that the feed solution is flown through it. Excluding the final data point for each test (under the assumption that an anomaly occurred and the membrane may have ruptured), both samples showed higher flow rates at all points along the experiment in the reverse configuration. Additionally, the standard sample had a student t-test value of 0.026 for these results, which is below the threshold value of 0.05 for it to be statistically significant. Additionally, the rejection rate of the samples was higher when they were oriented in the reverse configuration. For the xylem to be an effective filter, we want both a high permeability and high rejection rate, to produce the maximum amount of clean and potable water. These results suggest that, for final implementation, the xylem should be loaded into the hosing in the reverse orientation. Finally, it appears that fouling is a viable method by which, the cutoff particle size for the xylem can be decreased, allowing the membranes to remove more particles from the feed solution.

5. Rejection Rate vs. Sample Length

5.1. Purpose of Experiment

Other literature suggests that 1.0in xylem samples are extremely effective at rejecting particles larger than 100 nm, with an estimated rejection rate exceeding 99.9%.¹⁶ However, the pressure required to drive feed solution through a membrane is proportional to the length of the membrane. This means that decreasing the length of the xylem reduces the pressure required to operate the filter, either reducing the height of the column of fluid needed to power the filter through gravity fed flow, or reducing the size of the pump needed to drive it. In previous work, tests performed on the xylem were done using only 1.0in samples. This study attempted to determine if there was a minimum length beyond which the rejection rate remained constant or if for a given particle size there was a minimum cutoff length required to achieve complete rejection.

5.2. Red Dye & Xylem Sample Preparations

Two different dilutions of red ink were prepared for this test: 300x diluted and 1000x diluted. The red ink contained a distribution of particle sizes ranging from ~70 nm to ~500 nm. The particles also had a tendency to aggregate into larger masses on the order of ~3000 nm to ~9000 nm.¹⁶ In order to break up these agglomerations, the samples were both thoroughly mixed and then sonicated for ~20 seconds before filtration.

The xylem were prepared using the same procedure spelled out in 3.3 with a few minor changes. Instead of being cut to the standard length, 5 samples were cut into lengths varying from ~0.2 in to ~1.0 in. Additionally, no parafilm was used to secure the samples in the hosing. The shorter samples didn't have enough length extruding from the base of the tube to wrap the film around. So, for consistency, none of the samples in these tests were wrapped with the film. These were done one at a time in series. The sample was prepared and cut, flushed with 10 ml of de-ionized water, and then with 5 ml of red ink. Afterwards, the hosing was washed with organic compounds (methanol or ethanol) followed by water. Then, the next samples was tested in the same manner. This was to keep the samples from drying out while another sample was being tested.

5.3. Red Dye Rejection Rates

For the 1000x dilution series, each of the 5 samples was loaded with 5ml of feed solution and filtered at 10psi. The filtrate was collected in 20 ml glass vials placed below the hose. The same was repeated with the 300x dilution series. Below are samples of the filtrate placed in 10 ml glass vials organized in increasing length. Going from left to right we have the unfiltered feed solution all the way up through a 1.08in xylem sample. Through visual inspection, it appears that increasing the length of the xylem improves rejection rate.

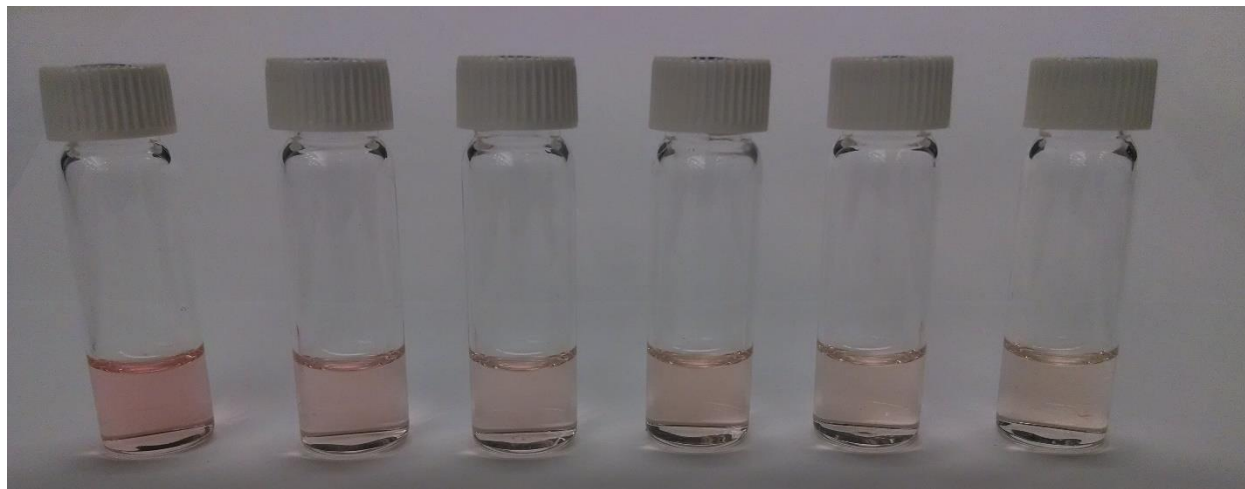


Figure 5-1 Filtrates showing rejection rate of dependence on xylem length for 1000x diluted red ink, from left to right: Unfiltered, 0.19in, 0.31in, 0.53in, 0.80in, 1.08in

To quantify the difference in rejection rates for each of the samples, an Agilent Technologies Cary 60 UV-Vis Probe was used to determine the light absorbance of each sample (see section 4.4 for a description of how the probe works). Again, 573 nm was chosen as the definitive peak at which the comparison would be performed. A calibration run was performed by using the unfiltered feed solution, measuring the absorption, diluting it 2x, 5x, and measuring the absorption of each of these concentration. Water was also measured as a control, which would simulate complete rejection. Then, the absorption for each of the filtrates was measured, plotted against wavelength, and the values at 573 nm were compared to determine if rejection rate increased with increasing length. The graphs for the calibration run and the actual filtrates are shown below.

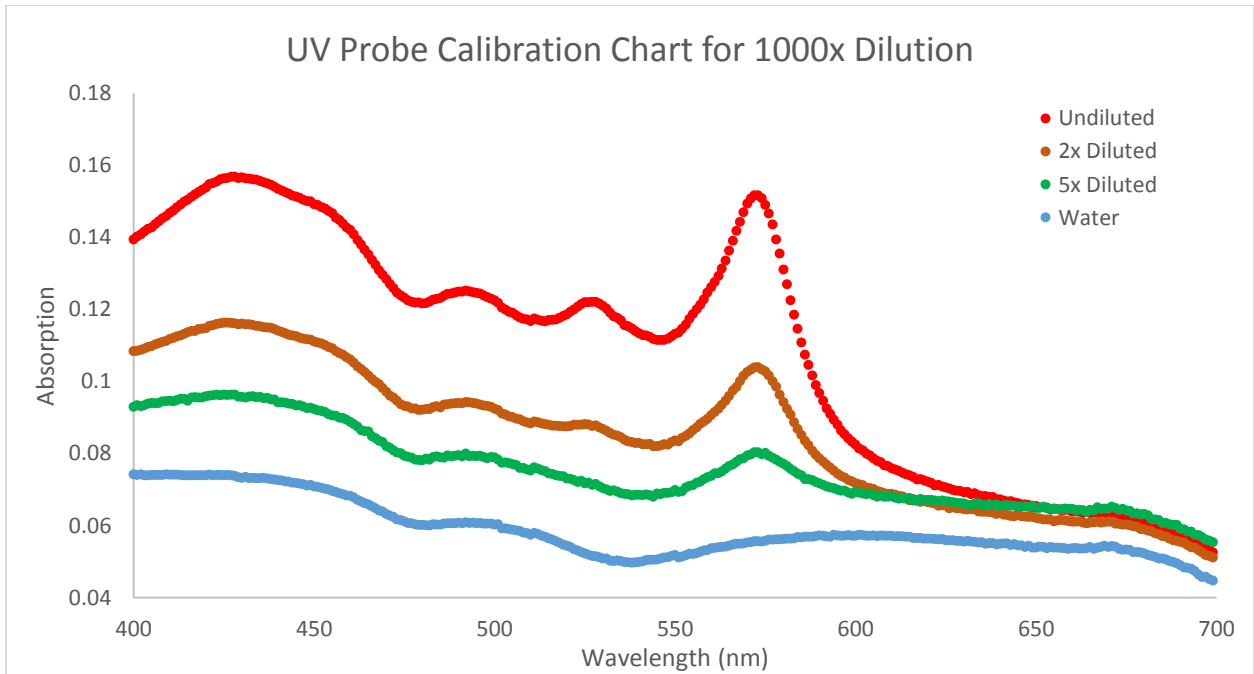


Figure 5-2 Absorption levels from scanning turbidity of 1000x diluted red ink, used as comparison to evaluate xylem rejection. Based on this graph, the defining peak used for comparison was chosen to be 573 nm.

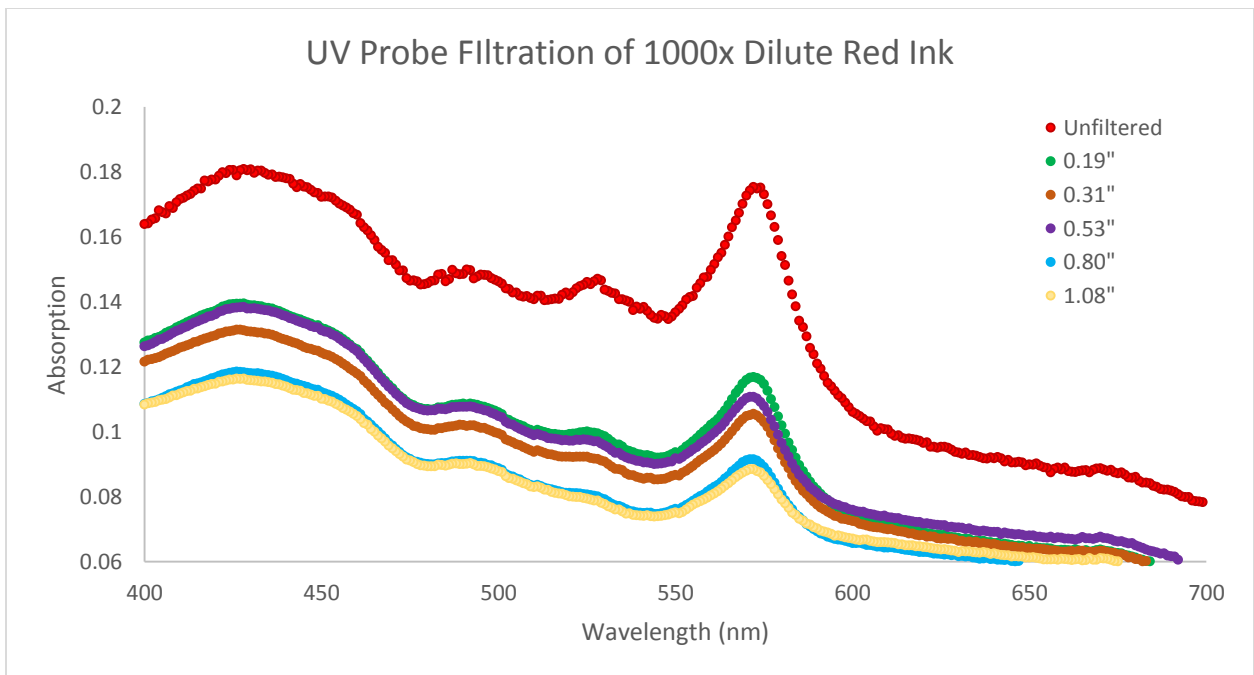


Figure 5-3 Actual absorption levels of the filtrate showing an increase in rejection rate as the sample length increases

Table 3 – Absorption values for the different sample lengths using 1000x diluted red ink for the feed solution

Sample	Absorption Value	Rejection Ranking
Unfiltered	0.0876	6 - Lowest
0.19”	0.0531	5
0.31”	0.0418	3
0.53”	0.0428	4
0.80”	0.0311	2
1.08”	0.0264	1

The same measurements and observations are repeated below for the 300x dilution series. Since the initial concentration was much higher, the calibration run included diluted solutions of 2x, 5, 10, and 100x dilution.

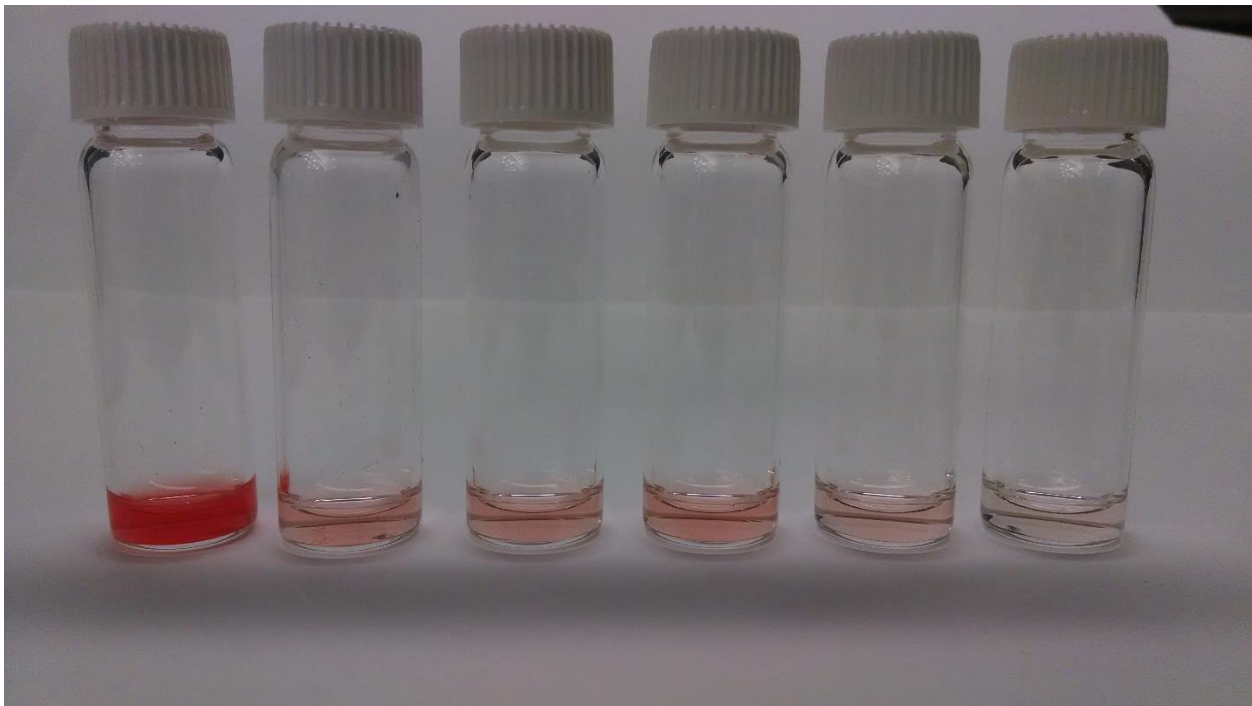


Figure 5-4 Filtrates showing rejection rate of dependence on xylem length for 300x diluted red ink, from left to right: Unfiltered, 0.20in, 0.31in, 0.57in, 0.79in, 1.09in

Cross sections of the five xylem samples used for the 300x dilution series are shown below. These show that the dye didn't penetrate any of the samples beyond the first 0.1 in. So, the pigment sizes that were filtered by the xylem were removed at the very top, while the smaller particles that could penetrate the xylem didn't appear to be filtered at a specific point along the sample.

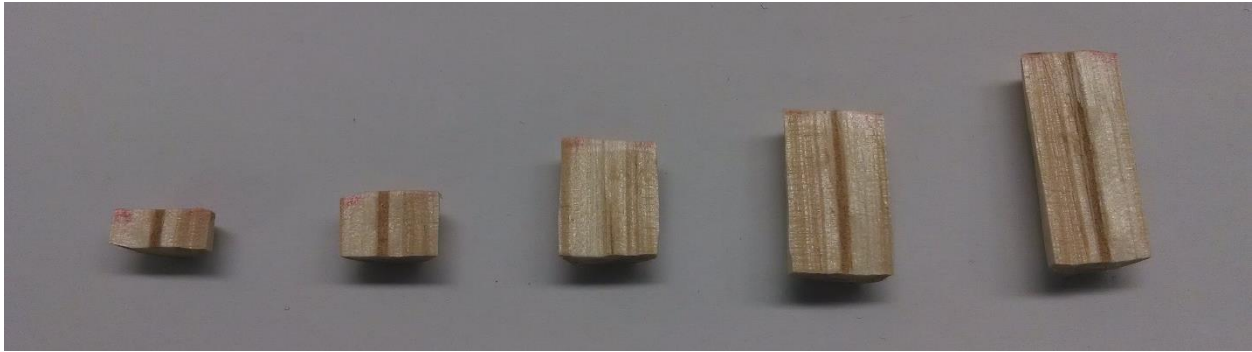


Figure 5-5 Cross sections of the xylem used for the 300x dilution filtration showing the ink not penetrating beyond the first 0.1in
 From left to right: Unfiltered, 0.20in, 0.31in, 0.57in, 0.79in, 1.09in

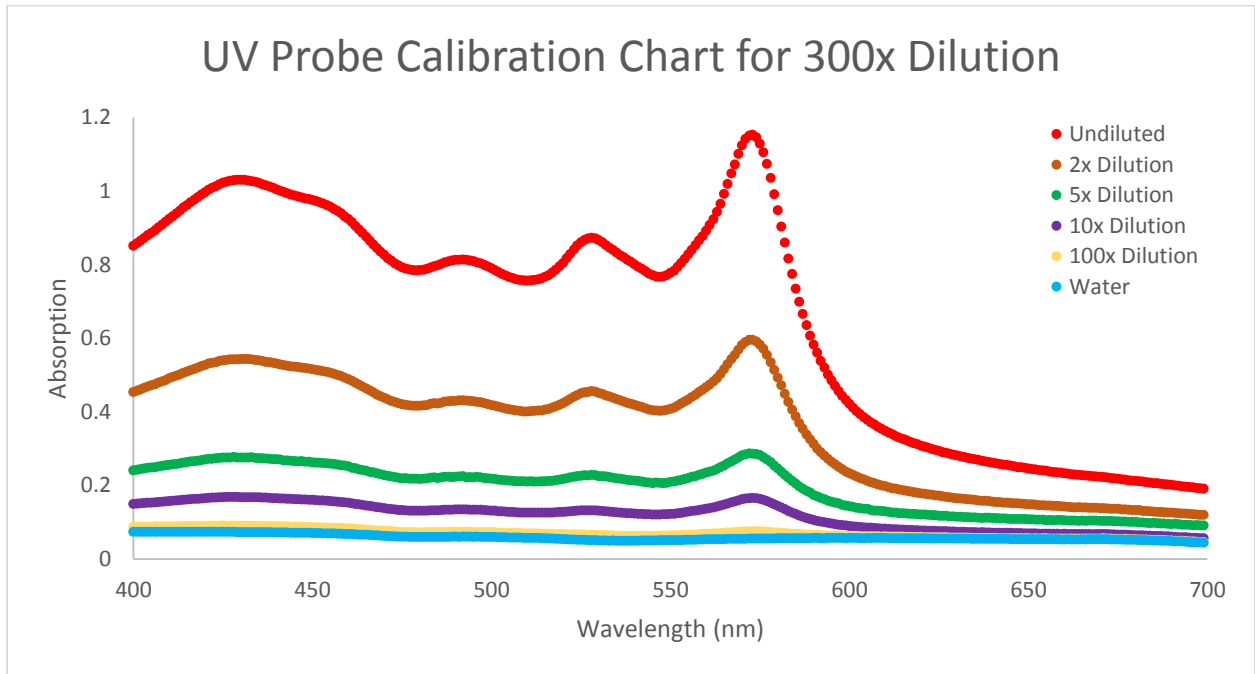


Figure 5-6 Absorption levels from scanning turbidity of 300x diluted red ink, used as comparison to evaluate xylem rejection
 Based on this graph, the defining peak used for comparison was chosen to be 573 nm.

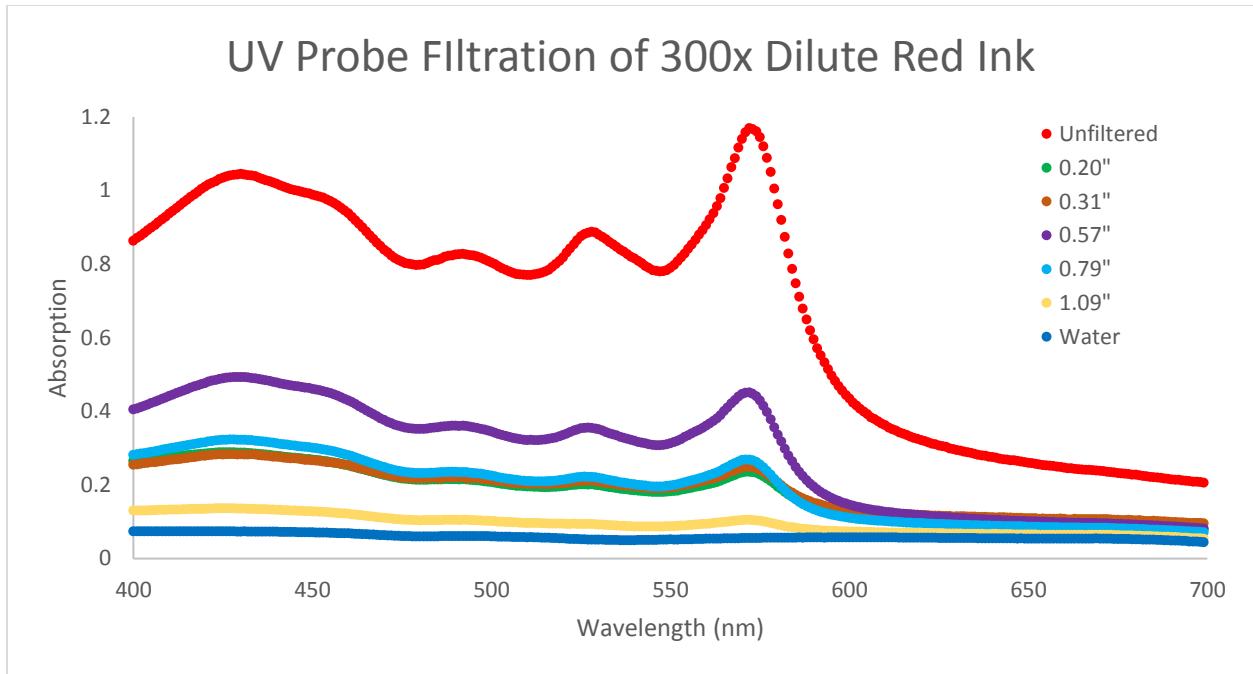


Figure 5-7 Actual absorption levels of the filtrate. There is no distinct trend for this data, which conflicts the results from the 1000x dilution series. This is a result of fouling changing the rejection rate since the feed solution was so concentrated.

Table 4 - Absorption values for the different sample lengths using 300x diluted red ink for the feed solution

Sample	Absorption Value	Rejection Ranking
Unfiltered	0.2173	6 - Lowest
0.20"	0.0292	4
0.31"	0.0250	2
0.57"	0.0525	5
0.79"	0.0267	3
1.09"	0.0068	1 - Highest

In the 1000x diluted red ink test, we see a general pattern of increased rejection with increased length. The exception to this is at the transition from the 0.53" to 0.80" samples where there is a slight increase in absorption. However, this is only a 2.3% increase, which may suggest that the rejection rates were the sample for these two samples. For the 300x dilution series, the rejection rate doesn't follow a nice trend like the 1000x series. In this run, the best rejection was with the longest sample; however, the intermediate samples showed similar rejection rates as the length changed. This was especially prevalent with the 0.20" 0.31" and 0.79" samples. Additionally, the rejection rate decreased from the 0.31" to 0.57" samples. At very high concentrations, a "cake layer" forms on the surface of the membrane that increases the resistance of the membrane to flow (see section 7.1 for additional details). The pores through the cake layer may be smaller than the pores in the xylem, allowing the combined xylem-cake-layer system to reject more particles. Additionally, since the red dye contains a variety of particles ranging from

70 nm (smaller than the xylem pores) to 500 nm (larger than the pores)¹⁶ some of the pores may be clogged or partially blocked with dye pigments, also increasing rejection.

5.4. Fluorescent Particle Sample Preparation

A solution of 1 μm FluoSpheres carboxylate modified orange fluorescent microspheres was chosen for this experiment and diluted using de-ionized water until reaching a concentration of $1.68\text{E}+06$ particles/ml 95% CI [1.54, 1.81]. This concentration was determined by enumeration with a hemacytometer (inCyto C-chip) mounted on a Nikon TE2000-U inverted epifluorescence microscope. An X-Cito wide-field fluorescence microscope excitation light source was used to produce a green light with a wavelength of 450 nm, which caused the particles to fluoresce for imaging.

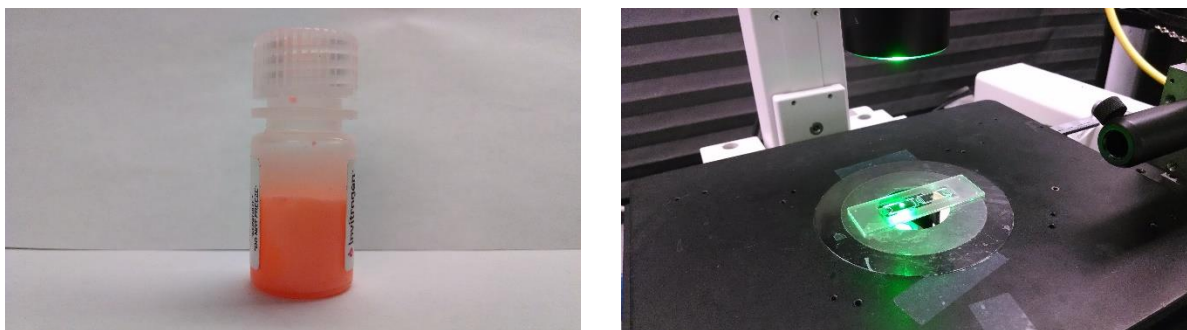


Figure 5-8 (Left) 1 μm fluorescent microspheres (Right) Microspheres being observed using 450 nm laser

An Andor iXon^{EM} + camera attachment on the microscope was used to take video and image the particles under 4x magnification on the c-chip with a 0.01 second exposure time on the lens. The still image was then used to count the number of particles within each box.

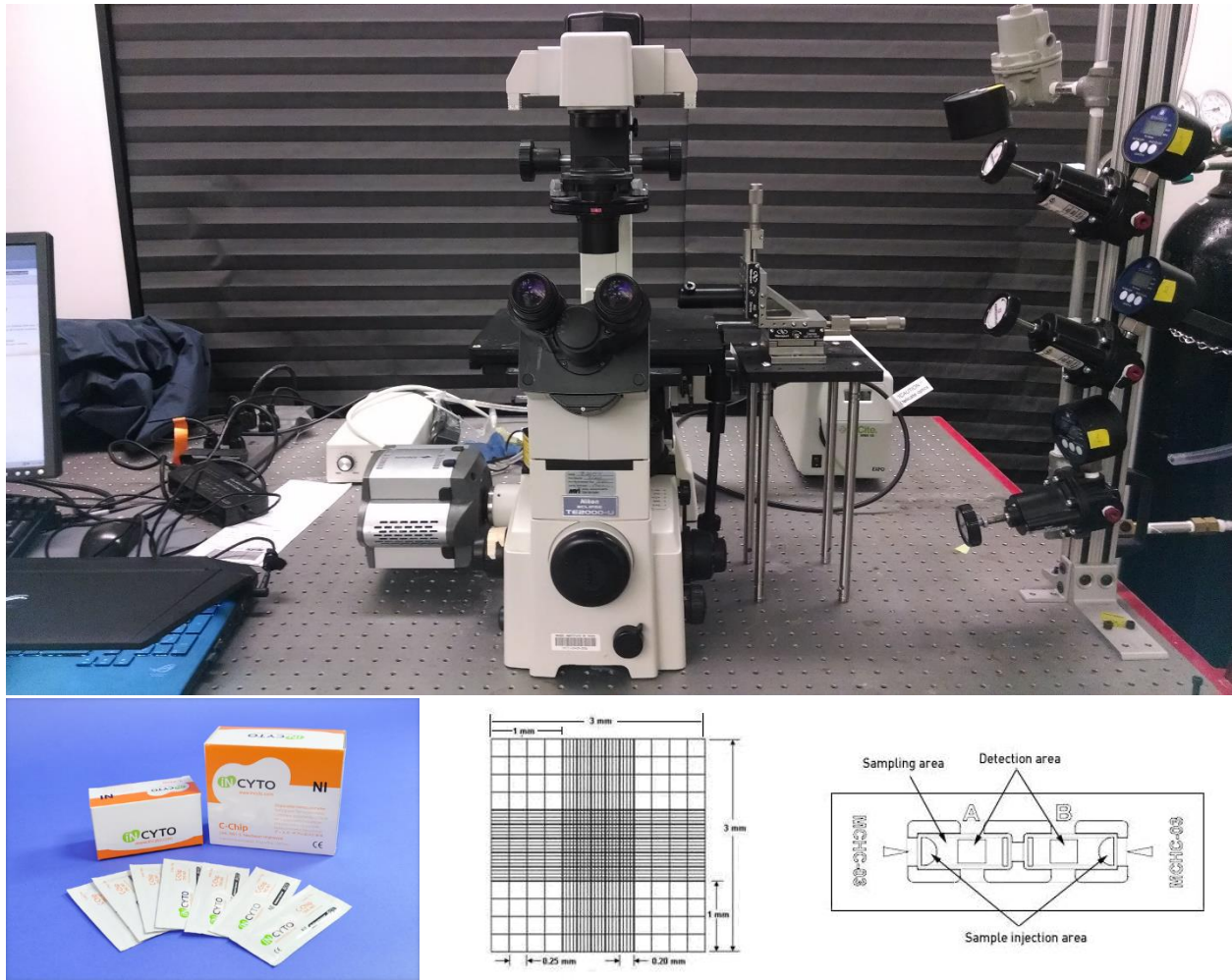


Figure 5-9 (Top) Nikon TE2000-U inverted epifluorescence microscope with X-Cito laser generator and Andor iXon^{EM} + attachment (Bottom Left) inCyto C-Chip used for enumeration (Bottom Right) Diagram of C-Chip

For these experiments, the four 1 mm² corner arrays were used to determine the concentration (see Figure 5-9 (Top) Nikon TE2000-U inverted epifluorescence microscope with X-Cito laser generator and Andor iXon^{EM} + attachment (Bottom Left) inCyto C-Chip used for enumeration (Bottom Right) Diagram of C-Chip). The number of particles in each individual square was counted and the total for each square was summed across the array. Then, the average of the four corner arrays was determined, along with the 95% confidence interval, and multiplied by the scaling factor of 10⁴ to get the number of particles per ml. This concentration was chosen because it was high enough that a large number of particles appeared on the c-chip but not too many that they couldn't be counted accurately. The solution was thoroughly mixed and sonicated both before filtration and before being placed on the c-chip for observation.

5.5. Fluorescent Particle Rejection Rates

The same procedure was followed for testing the xylem as in section 5.2, except the 1 μm particle solution was substituted for the red dye. The concentration of the particles was determined through the same process by which we set our initial concentration in section 5.4. Below are images taken of the unfiltered feed solution, and two of the samples (0.1” and 0.25” in length).



Figure 5-10 Fluorescent microsphere concentrations in (Left) unfiltered feed solution (Middle) filtrate from 0.10in sample (Right) filtrate from 0.25in sample. This suggest that the minimum length to rejection 1 μm is 0.25in. (Not Shown) filtrates from the 0.41in, 0.51in, 0.77in, and 1.00in because they were identical to the 0.25in filtrate. Each box is 0.25mm x 0.25mm.

5.6. Conclusion

Since the pores for the xylem are on the order of 100nm in diameter,¹⁶ we would expect particles larger than that to be completely rejected so long as there isn't one continuous tracheid acting as a through path through the membrane. There needs to be at least one "pit" on each pathway to filter out the particulates. This was shown with the 1 μm microspheres where no particles were observed in the filtrate of the 0.25in sample and beyond that. Even with the 0.1in sample, the xylem was able to reject 98.2% with a 95% CI of [97.0%, 99.3%]. This means that xylem samples greater than or equal to 0.25in in length are effective at filtering bacteria. This is further confirmed by the images taken of the cross section of the samples that were used to filter the 300x dilution red ink. The samples show that the ink didn't penetrate beyond the first 0.1in, which was confirmed by comparing my results against previous work.¹⁶

On the other hand, for particles smaller than 100 nm, we observe that rejection rate improves with increasing membrane length from the 1000x diluted red ink tests. So depending upon the particulate size in the feed solution, the length of the xylem may or may not have an effect on your rejection rate, where the cutoff is around 100 nm.

6. Charles River Water Filtration

6.1. Purpose of Experiment

The major potential use for which we are testing the xylem, is in being implemented as a low cost, biodegradable filter for personal use in developing countries. We see the most likely use scenario being a person gathering water from the edge of a river, pond, or other water source and filtering it for drinking, cooking, cleaning, etc. Therefore, the xylem's performance at filtering particulates from a naturally contaminated water source was essential to quantify and properly evaluate the feasibility of this solution.

6.2. Gathering Sample & Preparation

The setup for this test followed the general preparation procedures in section 3.3 to the letter. Feed water samples were gathered from the bank of the Charles River in Cambridge, MA for testing. The samples were taken from the Cambridge side shore across the street from 471 Memorial Drive. Before filtration, the samples were stirred vigorously; however, they were not sonicated to better replicate the condition they would be found in nature.

6.3. Filtration Results

In each of these experiments, 5ml of Charles River water was filtered using the xylem samples. The filtrate was collected in 20 ml glass vials placed below the hose. Below is a side-by-side comparison of the two vials, before filtering and after, as well as a view of the retentate that was filtered by the xylem. Similar to the dye rejection, the Charles River particulates do not appear to penetrate beyond the first 0.1 in of the xylem, adding more support to the theory that most of the rejection occurs at the beginning of the sample.

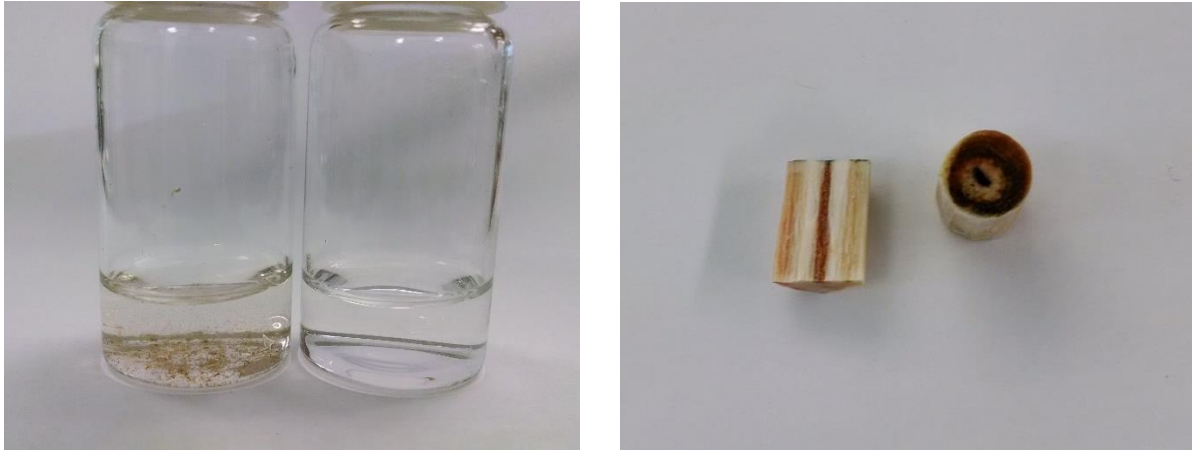


Figure 6-1 (Left) Side by side comparison of unfiltered and filtered Charles River water (Right) the xylem after filtration with a cake layer of retentate built up on the top surface

The turbidity of the samples was also observed using the Cary 60 UV-Vis probe, the results are shown below. From the graph, we can see that both samples rejected a significant number of particles from the solution. Additionally, all 4 of the solutions that were tested showed similar curve shapes across the spectrum of wavelengths scanned. This means that there wasn't a high concentration of dissolved particles in any of the filtered solutions. However, neither of them was able to bring the absorption level down to the same point as water.

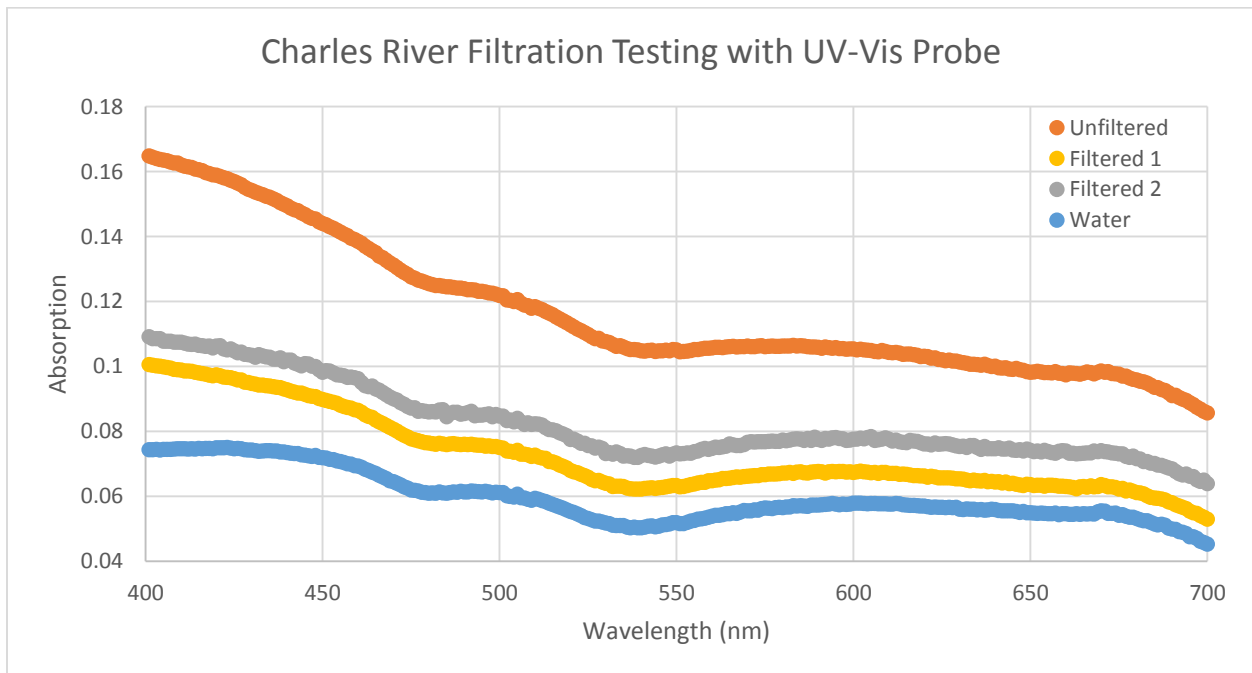


Figure 6-2 Absorption curves for the solutions used in testing the xylem's ability to reject Charles River water

For more detailed examination of the xylem's ability to filter the Charles River water, the two samples were compared using a hemacytometer (inCyto C-chip) mounted on a Nikon TE2000-U inverted epifluorescence microscope (see section 5.4 for description of C-chip). Below is a side-by-side comparison of images taken from the microscope.

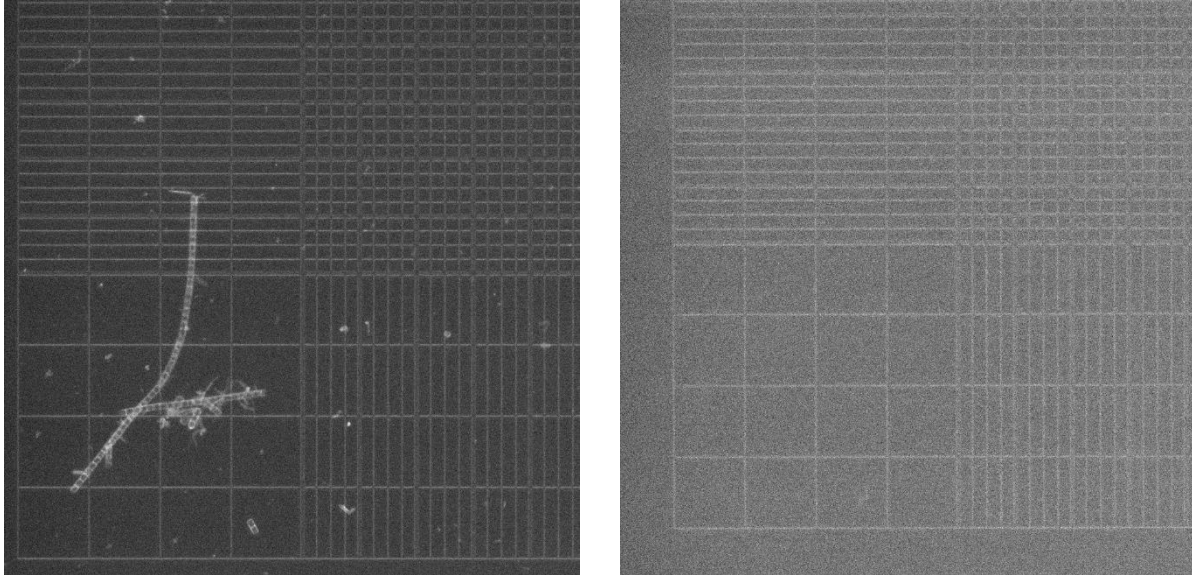


Figure 6-3 (Left) Unfiltered Charles River water observed on a C-Chip (Right) Filtered Charles River water. Each image covers a 2.0mm x 2.0mm box.

6.4. Conclusion

The Charles River filtration served as a real-world test scenario to determine the xylem's performance as a filter for individual user application. Upon visual inspection, comparing the feed solution with the filtrate, the xylem removed a significant number of particles from the river water. The xylem also significantly reduced the turbidity of the river water, which was quantified using the Cary 60 UV-Vis probe. This was later confirmed by comparing them under a microscope, where it appears that the xylem completely rejected all large scale particles that could be seen using visual inspection with the Nikon microscope from the river water. This offers promising support to the plausibility of the xylem as a low-cost filter to provide potable water in developing countries.

7. Filtration Fouling Testing

7.1. Purpose of Experiment

One of the main drawbacks of dead-end membrane filtration is that the permeability of the membrane can decrease as more particles are filtered from the feed solution. This is a result of several mechanisms including:

- *Complete Blocking*, which assumes a seal of pore entrances and the prevention of any flow through them. As pore entrances are sealed, the area open to flow is reduced.¹¹
- *Intermediate blocking*, which assumes a seal of pore entrances by a fraction of particles and a deposition of the rest on the top of them.¹¹
- *Cake filtration*, which is a mechanism by which particles accumulate at the surface in a permeable cake of increasing thickness that adds a hydraulic resistance to filtration.¹¹
- *Standard Blocking*, assumes an accumulation inside the membrane on the pore walls. As the pores are constricted, the membrane permeability is reduced.¹¹
- *Concentration polarization*, as the solute is completely or incompletely retained by the membrane, it accumulates at the membrane surface, developing a boundary layer along the channel. This greatly affects the separation performance when the solute separation is incomplete.²

This experiment was aimed at characterizing how the xylem's performance degrades over time to see whether there exists a maximum amount the xylem can filter before it is no longer permeable.

7.2. Sample Preparation

The xylem preparation for this test followed the general preparation procedures in section 3.3 to the letter. For the red dye, this test was initially carried out using a 5,000x diluted solution (volume/volume) in 5 ml increments; however, this proved to be too much retentate in a given step for accurate mapping of the drop in permeability as particulates were filtered from the feed solution. The flow rate decreased too drastically over the course of filtering the 5 ml of dye, so the step size was decreased to 1 ml of feed solution and the dye was further diluted to 20,000x dilution (volume/volume). As with all dye samples, it was thoroughly mixed and sonicated before filtration. The same Charles River sample was used as in section 4, again the solution was thoroughly mixed before each filtration but not sonicated. De-ionized water was used as a control in this test.

7.3. Fouling Results

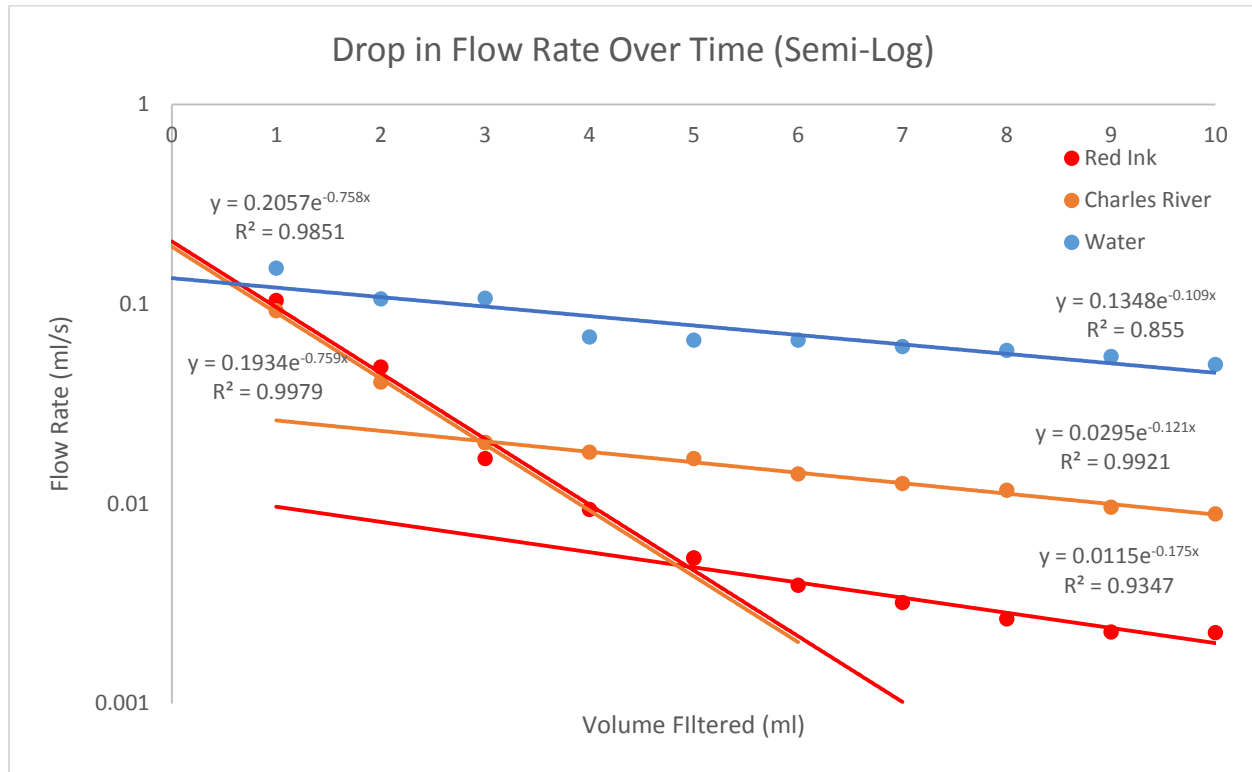


Figure 7-1 Graph showing how flow rate declines with cumulative volume filtered due to membrane fouling for de-ionized water, Charles River water, and red ink. For solutions with dissolved particles, there is a clear transition point between an initial sharp decrease in flow rate and a steady state decline that is also shown in the control. As expected, the red ink had the most dramatic decrease and the Charles River water was between the water and ink.

In the semi-log plot above, we see that for all feed solutions, even the de-ionized water, caused a decrease in flow rate over time. Interestingly, the solutions with dissolved particles in them, the red dye and Charles River water, have a much sharper drop in flow rate very early on, before leveling out to a more gradual decrease. This transition from a steep transient to a more gradual steady state happens at a clear bend in both curves. For the red dye it's at 5 ml of cumulative solution filtered, and for the Charles River it's at 3 ml. Once they've leveled out, the two lines closely resemble the curve for the de-ionized water. This suggests that different fouling mechanisms are dominant during different regimes on the graph.

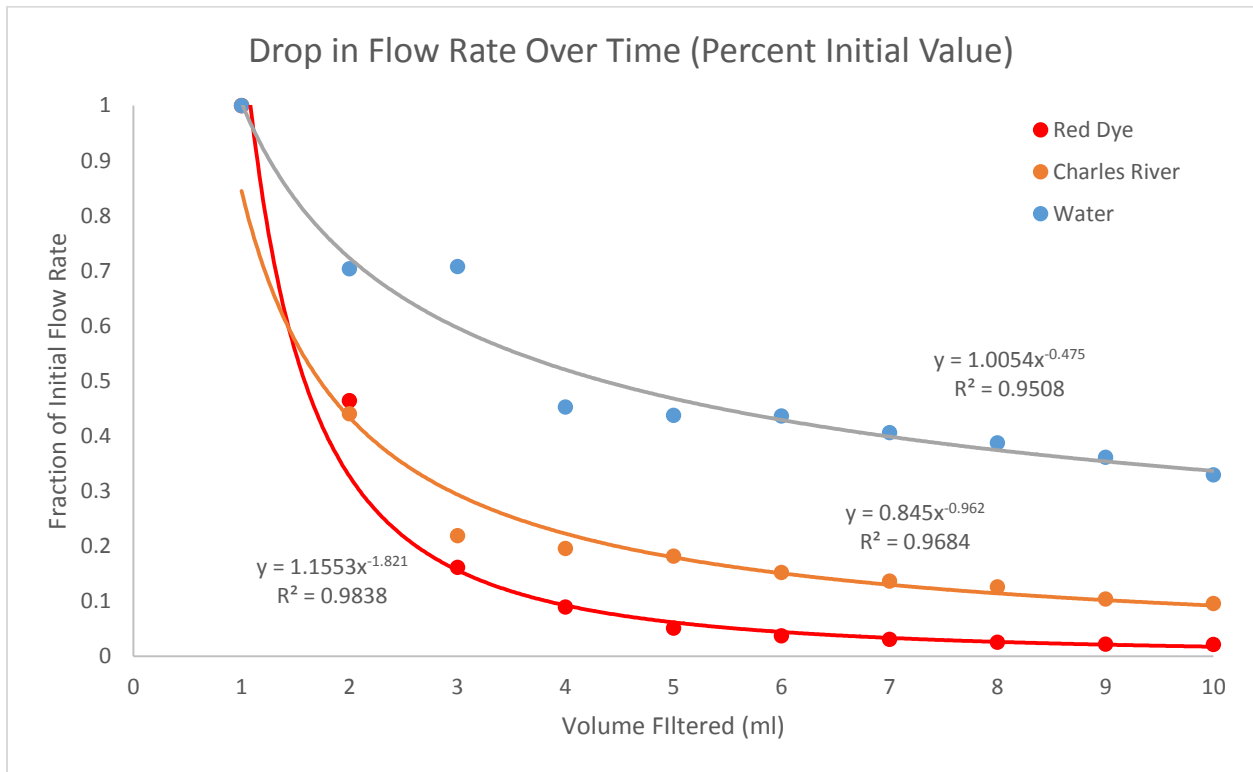


Figure 7-2 Graph showing the drop in flow rate due to fouling normalized by the initial flow rate. As expected, water had the least effect on the flow rate of the xylem, while the red ink, which was the most concentrated solution, had the greatest effect.

The graph above shows the decline in as a percentage of the initial flow rate. As expected, the de-ionized water declined the slowest and had the smallest drop in magnitude. The red dye, which had the highest concentration, declined the fastest and dropped to the lowest steady state value of the solutions. This graph uses power law relations to fit curves to the data points. For a constant pressure filtration, the mechanisms discussed in section 7.1 (complete blocking, intermediate blocking, cake filtration, and standard blocking) can be modeled in a common frame of power-law relationships using the format:¹¹

$$\frac{d^2t}{dV^2} = k \left(\frac{dt}{dV} \right)^n \quad (2)$$

Table 5 – Table of various fouling mechanisms with their governing equations and physical depictions¹¹

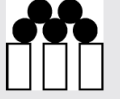
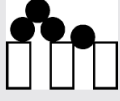


Fouling mechanism	n	Corresponding linear form	Physical concept
Cake filtration	0	$\frac{dt}{dV} = \frac{1}{Q} = f(V)$	Formation of a surface deposit 
Intermediate blocking	1	$\frac{dt}{dV} = \frac{1}{Q} = f(t)$	Pore blocking + surface deposit 
Standard blocking	1.5	$\left(\frac{dV}{dt}\right)^{1/2} = Q^{1/2} = f(V)$	Pore constriction 
Complete blocking	2	$\frac{dV}{dt} = Q = f(V)$	Pore blocking 

Table 5 above summarizes the governing equations and has depictions of what is physically happening to the membrane for each fouling mechanism. More specifically, the permeate flux, J , with filtration time can be modeled by a classical Darcy law:¹¹

$$J = \frac{\Delta P}{\mu R} = \frac{\Delta P}{\mu(R_m + R_c)} \quad (3)$$

Where R_m and R_c correspond to the hydraulic resistances of the filter (fouled or not) and the hydraulic resistance of the cake, respectively. When complete blocking is one of the mechanisms at work, we can model the fouling using the following equation:¹¹

$$R_{m,\beta} = \frac{R_{m,0}}{1 - \beta_B} = \frac{R_{m,0}}{1 - \eta_B \left(\frac{V}{A_0}\right)} \quad (4)$$

Where $R_{m,0}$ is the clean membrane hydraulic resistance, V is the cumulative permeate volume, β_B is the surface coverage ratio of the membrane (which is increasing with V), A_0 is the initial surface area, and η_B is the blocked surface area by unit of time and surface of the membrane.¹¹ The cake hydraulic resistance, R_c , increases with cumulative permeate volume, V , according to the following equation:¹¹

$$R_c = \frac{\eta_c}{A_0} V \quad (5)$$

where η_c is the volumic specific resistance of the cake. Finally, for internal fouling, the filter resistance again increases with with cumulative permeate volume, V , according to the standard blocking law:¹¹

$$R_{m,I} = \frac{R_{m,0}}{1 - \eta_I V^2} \quad (6)$$

where η_I is the volume of particle accumulated in the media per unit of permeate volume and per unit of void volume.¹¹

7.4. Conclusion

As with all dead-end filtration setups, the xylem filter is susceptible to fouling, and so the permeability of the xylem decreases with continued use. It has been shown that the mechanism by which the xylem fouls depends greatly on the feed solution, specifically the size of the dissolved particles that are being retained. However, for all dissolved solution that were tested, there appear to be two regimes of fouling that occur. Initially, there is a sharp decrease in permeability, which is followed by a sudden switch to a more gradual decrease in the steady state. This suggests that different mechanisms may dominate at different points in time with the same sample and feed solution. The fact that these xylem-feed solution combinations all appear to eventually reach a point where the decrease in flow rate occurs slower than initially, we can account for this change and scale the sample up to provide the desired flow rate for a longer period of time. For example, with the Charles River water, we see that this plateau starts after 3 ml of cumulative fluid filtered. From this point until the end of the test, the flow rate was between 10%-22% of the initial flow rate. So, to have our desired flow rate in the steady state, we would need to increase our cross-sectional area by roughly a factor of 9x. Since the area scales with the diameter squared, we would simply need to triple the diameter of the sample we used. For the red dye, the steady state was around 2% of the initial flow rate, which would need a 7x larger diameter sample to have the desired flow rate in steady state.

8. Preservation Techniques

8.1. Purpose of Experiment

The premise of this study was to coat the surface of the tracheids using a polymer solution, which, after drying, would form a layer between the Torus and Margo of the “pit” membrane that makes the wood porous and allows filtration (see section 2.2 for more detail on xylem structure). That way, when the xylem dried out, the “pit” would rest on the layer of polymer instead of irreversibly sticking to the membrane. Then, water could be flown through the xylem again, passing through gaps between the polymer chains, rewetting the xylem and raising the “pit” back into its initial position.

8.2. Background & Theory

The xylem samples were empirically determined to have an average of 61.49% water composition 95% CI [60.18, 62,80]. Freshly cut samples were massed using a Mettler Toldo AL104 scale and left to dry for several days. They were then reweighed and the water composition was determined by the change in mass. Previous work has shown that the xylem’s permeability and ability to reject particles is highly dependent upon remaining wetted. In those studies, samples that were left to dry for several hours showed irreversible drops in flow rate by factors of over 100.¹⁶ Several techniques were tested to reverse this effect, including wetting using ethanol or vacuum to remove air.¹⁶ None of these had any significant effect on the flow rate, suggesting that the pit membrane may have a tendency to become clogged during drying.¹⁶ This is consistent with literature, which shows that the pit membranes can become irreversibly aspirated against the cell wall, blocking the flow.²⁰ This section tests additional preservation techniques and discusses their effectiveness at retaining both permeability and rejection capability.

8.3. Polymer Research, Selection, & Solution Preparation

For the coatings, I chose to test Polyvinylpyrrolidone (PVP), dish detergent, and glycerol. Our criteria for selecting coatings were that it needed to be non-hazardous, stable at room temperature, and either a liquid or a solid that could be dissolved in a liquid to be flushed through the xylem to coat the interior. The advantage of the PVP was that it is available in different polymer lengths. This allowed us to determine the effect the length of the coating molecule had on its performance. I chose three different lengths of PVP, where two of them were smaller than the cutoff length of 100 nm and one was larger. The shorter polymer lengths were chosen to allow them to pass through the filter and coat the interior of the tracheids and the area between the Torus

and Margo. The longer polymer length was chosen in case the shorter lengths were too small that they simply passed through the xylem without coating the surfaces.



Figure 8-1 (Left) Containers of glycerol & the 3 different polymer lengths of PVP (Right) PVP Monomer

Shown above is a monomer of the PVP polymer. The interatomic distance of a C-C bond is 1.54 Angstroms.³ Using this number, Table 6 – Summary of the different polymer lengths chosen for Polyvinylpyrrolidone (PVP) summarizes the lengths and costs of each of the different molecular weights.

Table 6 – Summary of the different polymer lengths chosen for Polyvinylpyrrolidone (PVP)

Molecular Weight	Number of Monomers	Length of Polymer (nm)	Cost
10,000	90	12.8	\$83.17/kg
40,000	360	51.2	\$170.40/kg
360,000	3,243	460.5	\$125.00/kg

The PVP solutions were prepared in 15 ml batches by dissolving the powder in DI water and stirring vigorously. Concentrations of 20%, 10%, and 5% by mass were chosen for the molecular weight 10,000 and 40,000 each to see if the coating concentration had an effect on its ability to preserve the xylem. For the molecular weight 360,000, a 1% concentration by mass was chosen due to the difficulty of dissolving a higher concentration of solid for that polymer length. A Mettler Toldo AL104 scale was used to measure out the proper amount of dry polymer that would be added to the water. Afterwards the solutions were thoroughly mixed on a VWR Analog Vortex Mixer until the polymers were completely dissolved. The following amounts were used:

Table 7 – Summary of the masses and volumes used to prepare the various concentrations of the PVP solutions

Concentration	Mass	De-Ionized Water
1%	0.15g	14.85 ml
5%	0.75g	14.25 ml
10%	1.5g	13.5 ml
20%	3.0g	12.0 ml

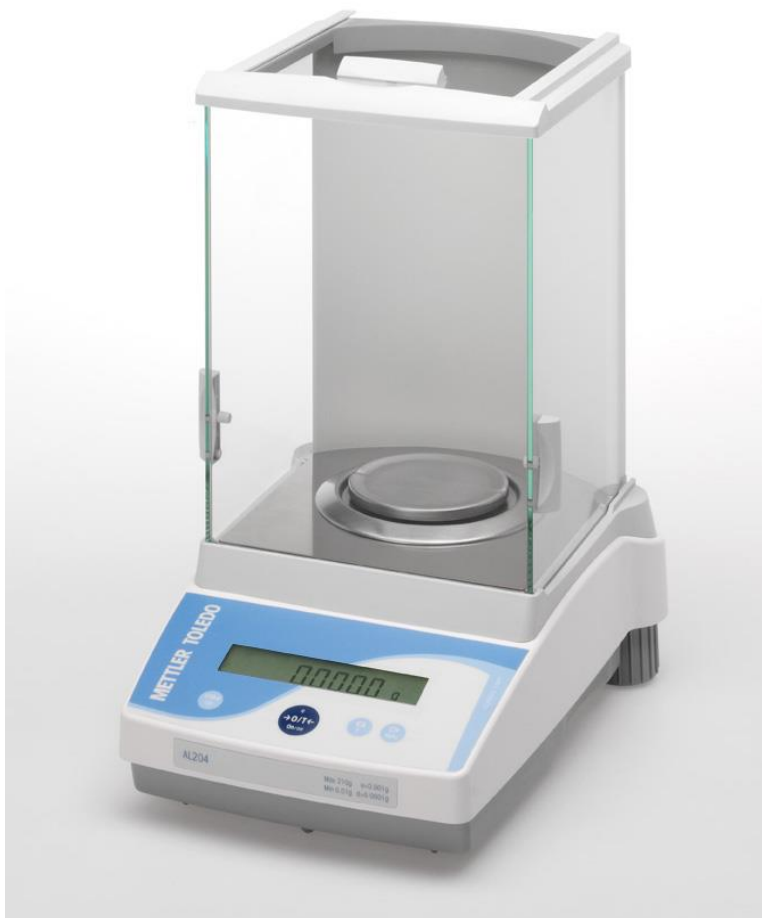


Figure 8-2 Picture of the Mettler Toledo AL104 scale used to prepare the coating solutions.

Both the dish detergent and the glycerol were too viscous to flow through the xylem in their concentrated states. Therefore, they were both diluted 5x by volume with de-ionized water and mixed thoroughly on an analog mixer. After the 5x dilution both coatings were able to penetrate the membrane under a pressure of 10 psi. Red ink was once again used to test rejection rate of samples. This time the sample was 1200x diluted, thoroughly mixed, and sonicated.

8.4. Testing Procedure

The xylem samples for this test followed the general preparation procedures in section 3.3. After being flushed with de-ionized water, each sample was then flushed with 1 ml of its respective coating and left to dry for ten days until all the water was removed. Initially, 13 samples were prepared using different polymers, polymer chain lengths, and concentrations. 1). Control that wasn't flushed with anything, 2). De-ionized water, 3). PVP molecular weight 10,000 at 5% (mass/mass), 4). PVP molecular weight 10,000 at 10% (mass/mass), 5). PVP molecular weight 10,000 at 20% (mass/mass), 6). PVP molecular weight 40,000 at 5% (mass/mass), 7). PVP molecular weight 40,000 at 10% (mass/mass), 8). PVP molecular weight 40,000 at 5% (mass/mass), 9). PVP molecular weight 360,000 at 1% (mass/mass), 10). Dish detergent, 11). Dish detergent 5x diluted (volume/volume), 12). Glycerol, and 13). Glycerol 5x diluted (volume/volume).

Once the samples were completely dried, each one was affixed to its own section of rubber tubing (roughly 5in long). A 5-minute cure epoxy was applied around the perimeter of each sample to seal it in the tubing. This precaution was taken because it was unclear whether the coatings would produce drastically different results. So even minor differences in flow rate may have been important in determining the optimal coating. Also, the samples shrunk during the drying process so they didn't fit as snugly inside the rubber tubing, which created a higher risk of leakage. After the epoxy cured, the end of the tubes were wrapped in parafilm. During testing, the connection point between the rubber tubing and the nitrogen tank line was also sealed using a hose clamp to prevent any leakage.



Figure 8-3 Modified experimental setup with hose clamp at connection between Nitrogen tank and xylem filter.

For testing procedures, a sample was chosen and flushed with 2 ml of de-ionized water. The flow rate was recorded, the same sample was flushed with an additional 2 ml of de-ionized water, and the process was repeated a total of 5 times. Then, the sample was flushed with 2 ml of the red ink and the filtrate was collected for later testing. This process was repeated for each of the 13 samples.

After testing the effectiveness of each coating on maintaining permeability and the rejection of particulates, the top coatings were chosen and retested. Again, the xylem samples were prepared following the general preparation procedures in section 3.3. After the sap was flushed from the samples with 10 ml of de-ionized water, the initial flow rate was measured using 5 ml of de-ionized water. This time, the coating solutions were sonicated before the samples were flushed using 5 ml of the coating and left to dry for two weeks.

8.5. Effect of Coating on Permeability after Drying

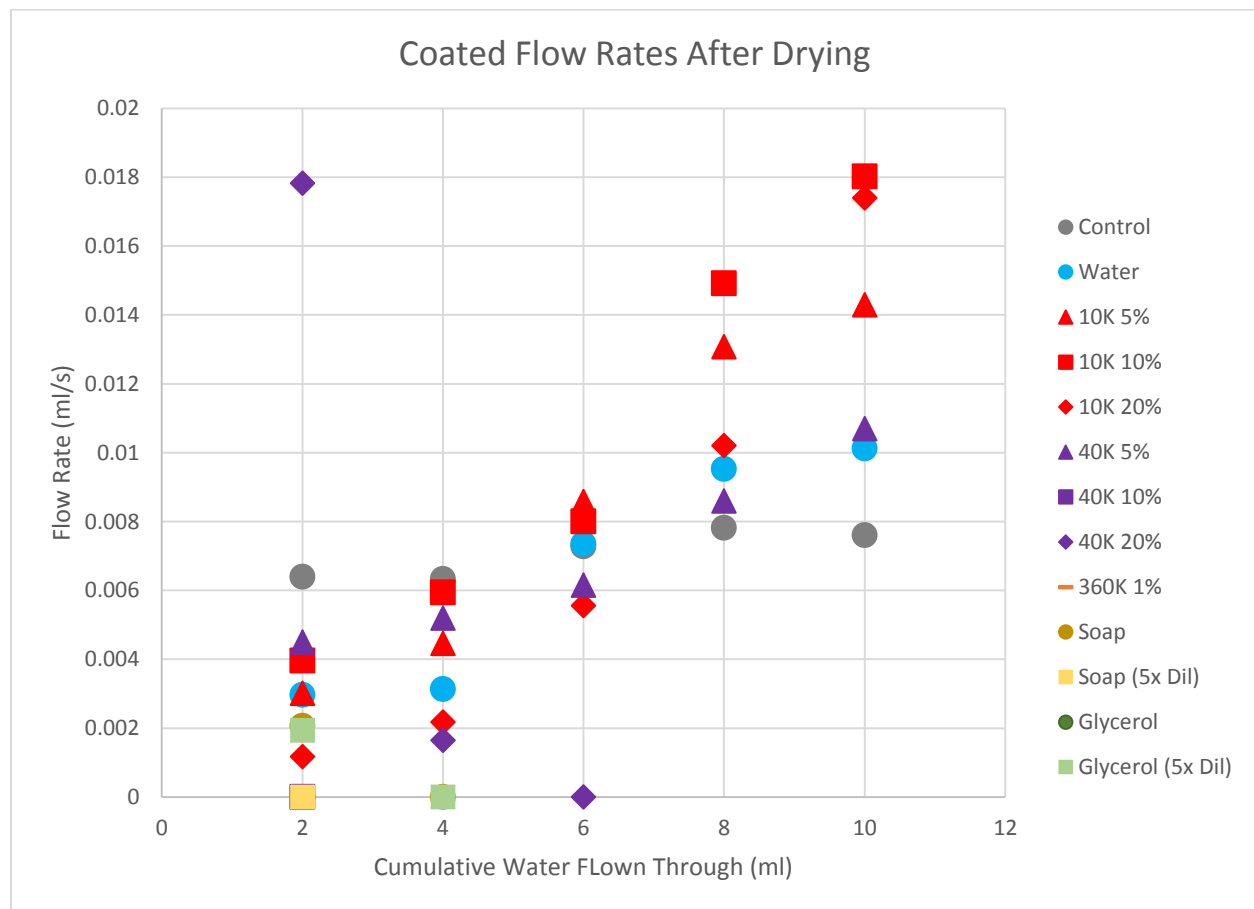


Figure 8-4 Graph showing the various coatings' performance at re-wetting the xylem once they've been dried. From these results the MW 10K and 40K PVP were selected as the best candidates for additional testing.

Above is a summary of the initial 13 samples' performance at preserving the xylem's permeability to determine the most effective coatings. From this graph, we can see that: soap, glycerol, and PVP molecular weight 360,000 all had little a negative impact on the sample's ability to rewet. The control, which was cut and left to dry without any coating or solution being flown through it, initially had the 2nd highest permeability; however, that value remained relatively constant as more water was flown through the sample. Similarly, the water produced permeability values in roughly the middle of the pack, with a slight increase in permeability as more water was flown through it. However, this also began to plateau at the end of the 10 ml.

By contrast, both the molecular weight 10,000 (at 5%, 10%, and 20%) and 40,000 (at 5%) solutions of PVP saw increasing permeability as more water was flown through them. Additionally, at the end of the final flush of de-ionized water, their values suggested a continuing upward trend in permeability, meaning they could achieve values even closer to the initial flow rate after additional use. The molecular weight 40K PVP (at 20% concentration) saw an extremely high initial flow rate, but sharply dropped off over time. I hypothesize that, since these samples weren't sonicated before coating, the polymers in this solution were stuck together in agglomerations too large to bypass the "pit" in the tracheids and were filtered out, building up a layer on the surface of the sample. Then, when water was flushed through it, these polymers broke free, were flushed into the sample, and then began to clog the pores. This would explain the sudden, dramatic decrease in flow rate. As a result, all coating solutions were sonicated before the second round of testing.

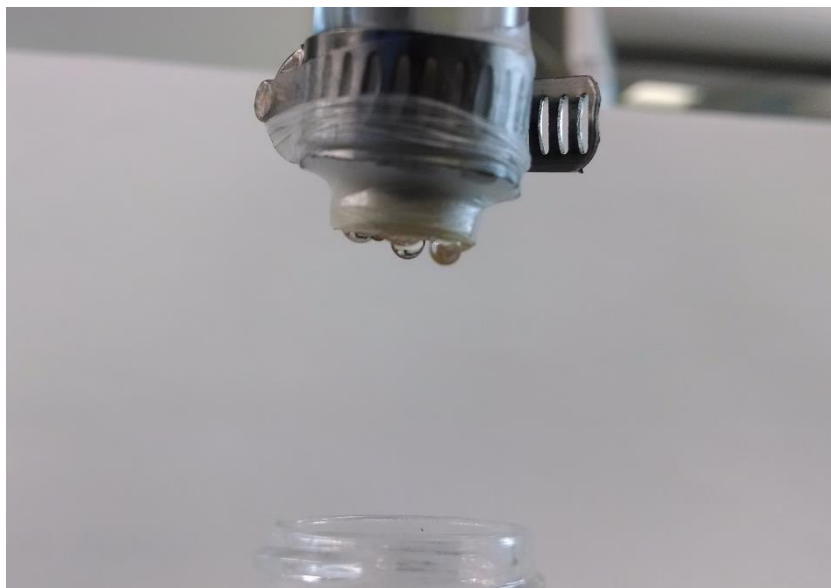


Figure 8-5 View of the base of a coated xylem sample during re-wetting test. There are individual channels within the sample that appear to allow flow through them while others appear blocked. This suggests that some, but not all, of the sample is re-wetting, meaning there wasn't enough coating flown through it initially.

Additional observation of the filtrate during permeability testing showed that the water traversed the membrane in several distinct spots and that some portions of the cross-sectional area didn't appear to allow flow through them. From the permeability graph shown above, we can see that the coatings helped preserve the sample's permeability after drying. Therefore, this suggests that some portions of the xylem cross-section were successfully coated, while others were not. As a result, the volume of coating solution flushed through the samples in the second round was increased from 1 ml to 5 ml.

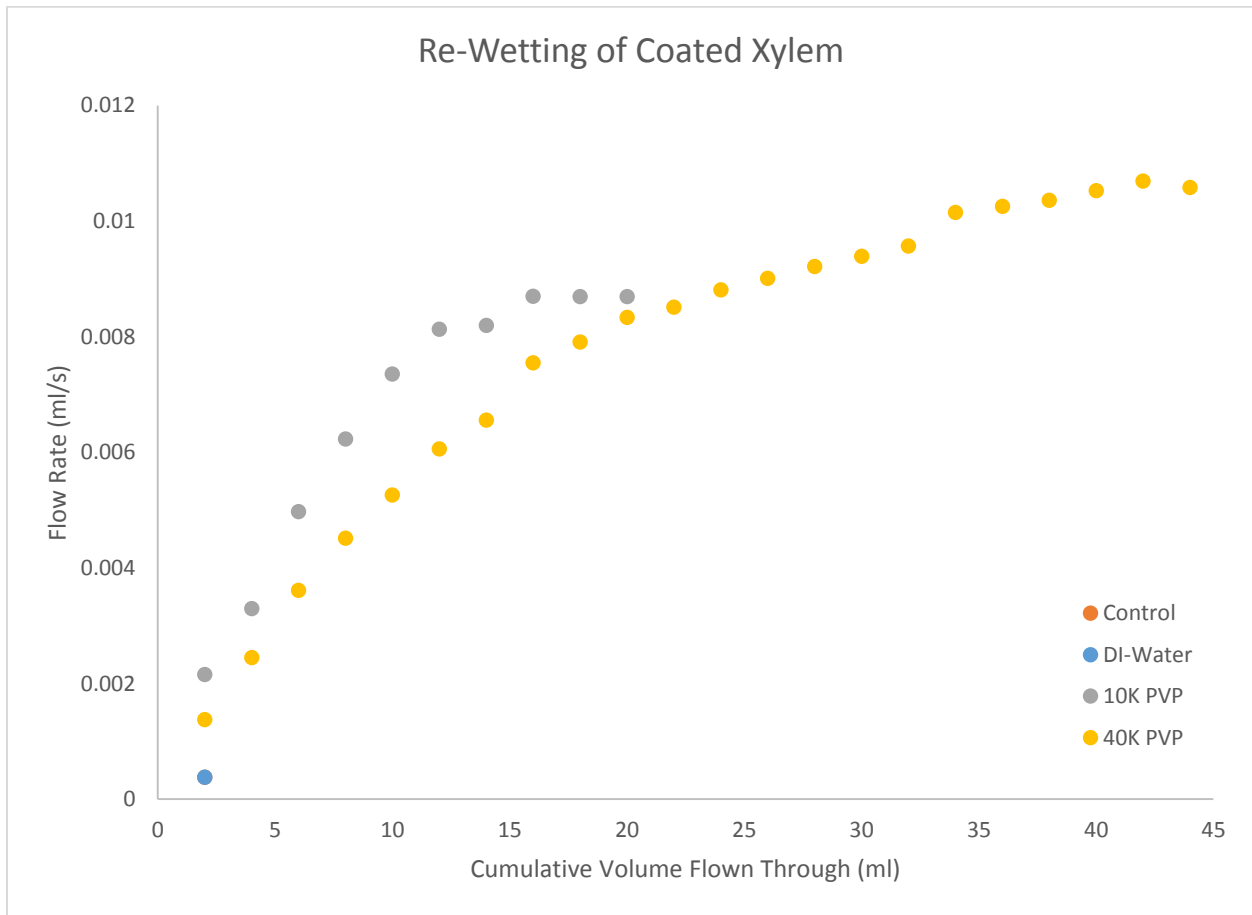


Figure 8-6 Graph showing how the coated and uncoated samples re-wet after drying for several days, note that measurements were taken until the flow rate for that sample plateaued. Additionally, the control & DI-water share the same initial point.

Above is a graph showing the second round of testing with the 4 samples: uncoated, de-ionized water, 5% MW10K PVP (mass/mass), and 5% MW40K PVP (mass/mass). These samples were left to dry for roughly 2 weeks before testing. Neither the control, nor the de-ionized water showed any signs of re-wetting. Roughly 0.5 ml of water was absorbed into the xylem at the start of the test, but afterwards the flow almost completely ceased. However, both the 10K and 40K PVP showed significant rewetting with time. After about 20 ml of cumulative water was flown through the sample treated with 10K PVP, the permeability returned to roughly 12.1% of its initial value before treatment and drying. Likewise, the 40K PVP coated sample returned to 14.7% of its

initial value after 44 ml of cumulative water. Both of these show promising results as potential coatings that can be used to preserve the samples for long periods of drying during transportation or storage.

8.6. Effect of Coating on Rejection Rate

In previous studies, some xylem samples were able to retain their permeability after drying; however, they lost the ability to reject particles.¹⁶ This may be attributed to the membranes becoming torn or damaged during the drying process. I tested to see if the samples that re-wet as a result of the PVP coatings also retained their ability to reject particles. After a xylem sample's permeability plateaued from re-wetting (after 20 ml for the 10K PVP and 44 ml for the 40K PVP), I flowed 2 ml of 5,000x diluted red ink through the sample. Below is a picture showing visual proof that the xylem was still able to reject the ink particles.



Figure 8-7 (Left) Unfiltered red ink at 5,000x dilution (Middle) Ink filtered using sample that was rewet after being coated with MW 10K PVP and (Right) MW 40K PVP

To further quantify this rejection, dynamic light scattering was performed using a Malvern Zetasizer Nano ZS. The distribution of particle sizes is presented below. We can see that all of the aggregated dye pigments with a size distribution centered on 5000 nm were completely filtered by the xylem. Additionally, the remaining particles that weren't filtered by the coated xylem were between 150-400 nm, centered on 220 nm. Both coatings maintained the xylem's ability to reject bacteria sized particles, and we do not see any discernable difference between the 10K and 40K PVP coatings.

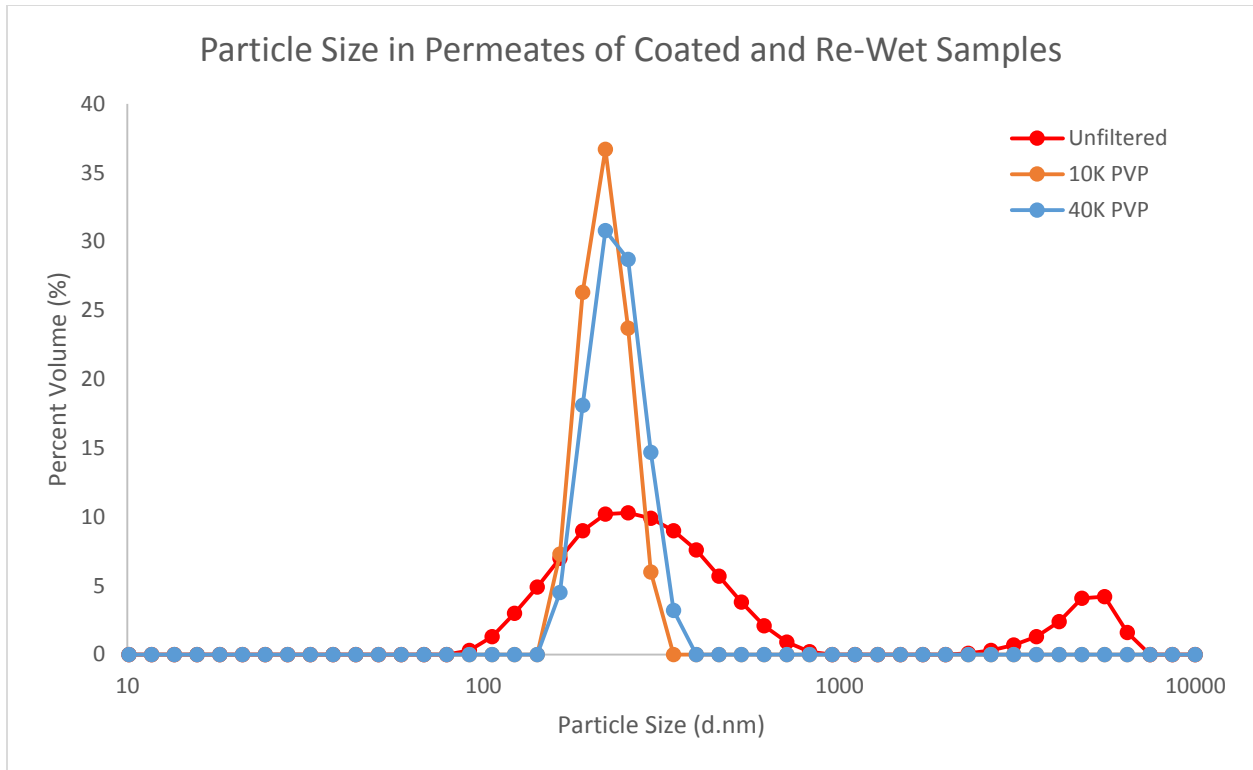


Figure 8-8 Particle size distribution of the permeates of the coated samples gathered using dynamic light scattering (DLS)

8.7. Conclusion

Both molecular weight 10K and 40K PVP showed promising results as potential coatings to solve the drying problem xylem face. The 10K PVP allowed the xylem to re-wet to 12.1% of its initial flow rate after flowing 20 ml of water through it, while the 40K PVP returned to 14.7% of the initial flow rate after 44 ml. This means that 10K PVP re-wet faster, but the 40K re-wet to a higher steady state permeability. This is compared to a roughly 1% retention of flow rate seen in the uncoated samples, which also exhibited no signs of re-wetting. After re-wetting, both coatings showed rejection rates comparable with fresh cut samples, suggesting they are still able to effectively filter bacteria from the feed solution. Another factor to consider is that the 40K PVP costs roughly twice as much as the 10K PVP. Additional testing should be done to see if there are more effective methods of coating the xylem than those tested in this paper.

9. Conclusion

It has already been shown in previous work that fresh cut xylem has a permeability of $\sim 5\text{-}6 \times 10^{-10}$ m²/Pa-s, can successfully reject >99.99% of *Escherichia coli* bacteria, and that a 1 cm² sample could provide enough drinking water in a day to meet an individual's needs.¹⁶ This paper continued evaluating plant xylem's potential as a low-cost, biodegradable, and readily available filter for providing potable water to the 1.1 billion people in need of it globally.

Commercially available clippers should not be used to prepare the samples. It was discovered during testing that these can cause undetectable cracks through the xylem in the axial direction that compromise its capability as a filter. These cracks only become visible once the sample has dried. Therefore, it is recommended that they samples be prepared using an industrial razor or a similar precision blade.

The xylem exhibited different permeabilities and rejection rates depending on the direction the feed solution was flown through it. To maximize both of these properties, the side of the xylem that normally faces the pine needles should be loaded into the hosing first. These differences were small but still statistically significant.

For bacteria and other particulates in the 1 μm range, a sample length of 0.25in was determined to be sufficient for complete rejection. Since the transmembrane pressure required to drive flow through the xylem scales with length, this would also be the optimal size for removing bacteria from the feed solution. However, for particles that are below the cutoff size of 100 nm, the rejection rate increased with the length of the sample. So, the optimal length of the sample is highly dependent upon the composition of your feed solution.

As a real world parallel, water from the Charles River in Cambridge, MA was filtered using the xylem. When observed under a microscope using a hemacytometer, the xylem appeared to remove many of the biological agents that were in the feed solution. Additional testing will need to be done to see if the smallest reagents, ones that aren't visible under a light microscope, were removed.

As with all dead-end filtration setups, the xylem filter is susceptible to fouling, and so the permeability of the xylem decreases with continued use. It has been shown that the mechanisms by which the xylem fouls depends greatly on the feed solution, specifically the size of the dissolved particles that are being retained. However, for all dissolved solutions that were tested, there appear to be two regimes of fouling that occur. Initially, there is a sharp decrease in permeability, which is followed by a sudden switch to a more gradual decrease in the steady state. All tests appear to eventually reach steady state transition point where the decrease in flow rate occurs slower than initially. We can account for this change and scale the sample up to provide the desired flow rate for a longer period of time. Additionally, it appears that fouling is a viable method by which, the

cutoff particle size for the xylem can be decreased, allowing the membranes to remove more particles from the feed solution.

Both molecular weight 10K and 40K PVP showed promising results as potential coatings to solve the drying problem xylem face. The 10K PVP allowed the xylem to re-wet to 12.1% of its initial flow rate after flowing 20 ml of water through it, while the 40K PVP returned to 14.7% of the initial flow rate after 44 ml. This means that 10K PVP re-wet faster, but the 40K re-wet to a higher steady state permeability. This is compared to a roughly 1% retention of flow rate seen in the uncoated samples, which also exhibited no signs of re-wetting. After re-wetting, both coatings showed rejection rates comparable with fresh cut samples, suggesting they are still able to effectively filter bacteria from the feed solution.

Overall, plant xylem from the Eastern White Pine, *pinus strobus*, shows remarkable potential as a low-cost, biodegradable water filter for developing countries to remove bacteria sized particles. The entire system can be powered entirely off gravity fed flow and scaled in size to accommodate both individual needs and supply potable water for a community. Additional testing will need to be done before this solution is fully implementable. However, based on its current performance, plant xylem is a strong contender worth looking into further.

10.Future Work

10.1. Other Species

This thesis focused solely on *pinus strobus* (white pine); however, there are numerous other types of trees out there that may work better for certain applications. *Pinus strobus* was a logical decision to use here at MIT because there are enough trees around that samples are readily available. However, this species of tree is only indigenous to the eastern portion of North America.²⁷ Therefore, if this is to become a global solution, local flora should be tested to ensure easy access globally. Additionally, the xylem pore size and tracheid length varies significantly across species, so some may have a higher permeability or lower cutoff length than white pine.

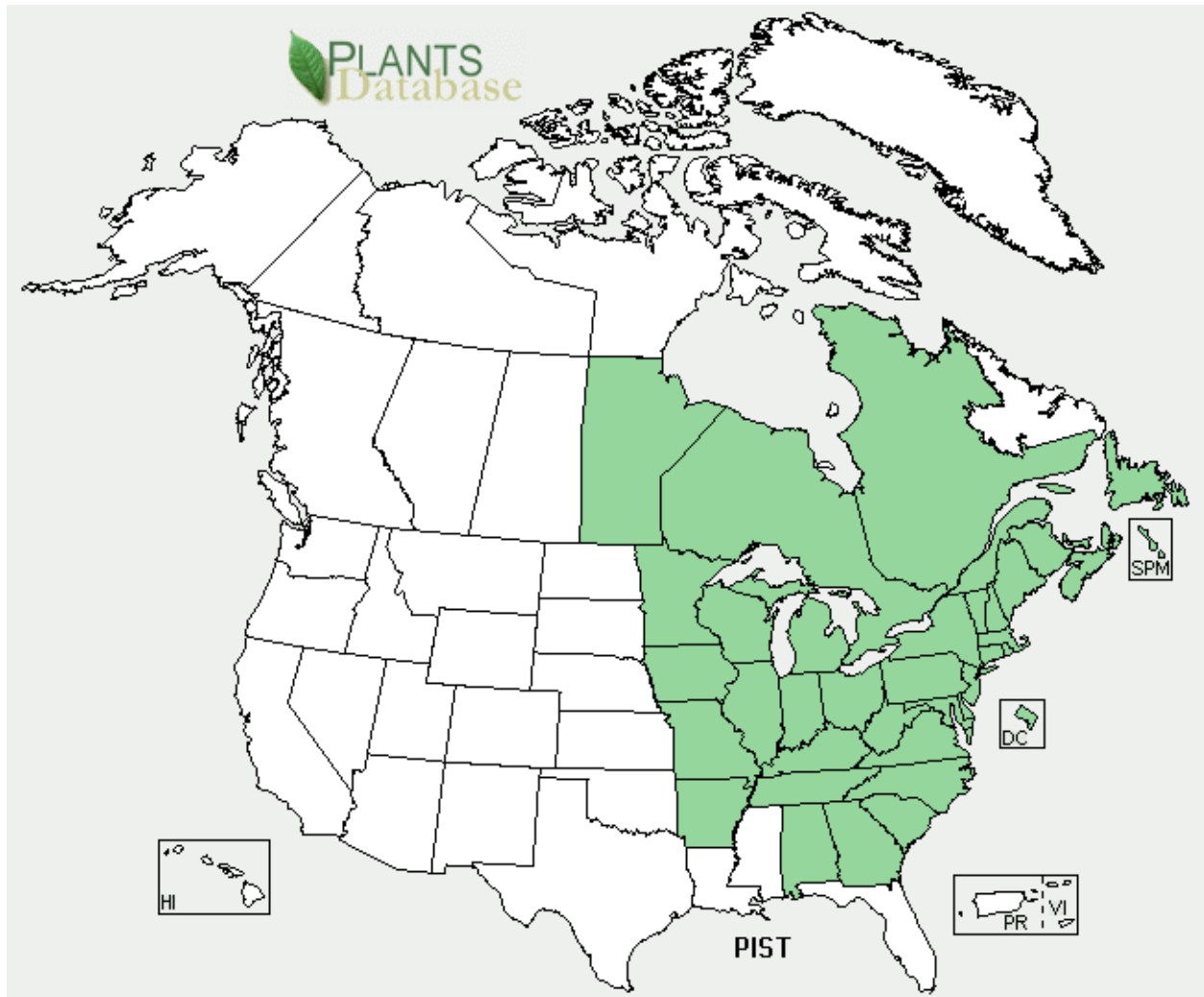


Figure 10-1 Map showing the indigenous regions of *pinus strobus* (Eastern White Pine)²⁷

10.2. Alternative Setups

The advantage to the setup used for these tests is that it is extremely simple and low cost. There are no moving parts and the entire system can be powered by gravitational flow; however, there are areas for improvement. Below is a diagram of a typical ultrafiltration membrane bioreactor (MBR). As you can see in the diagram, a pre-treatment system is usually implemented to remove much larger particles to help reduce fouling of the membrane. In our setup, this could be a simple coffee filter or another cloth membrane that would be responsible for removing the larger particles, so the xylem would only be required to filter the smaller ones.

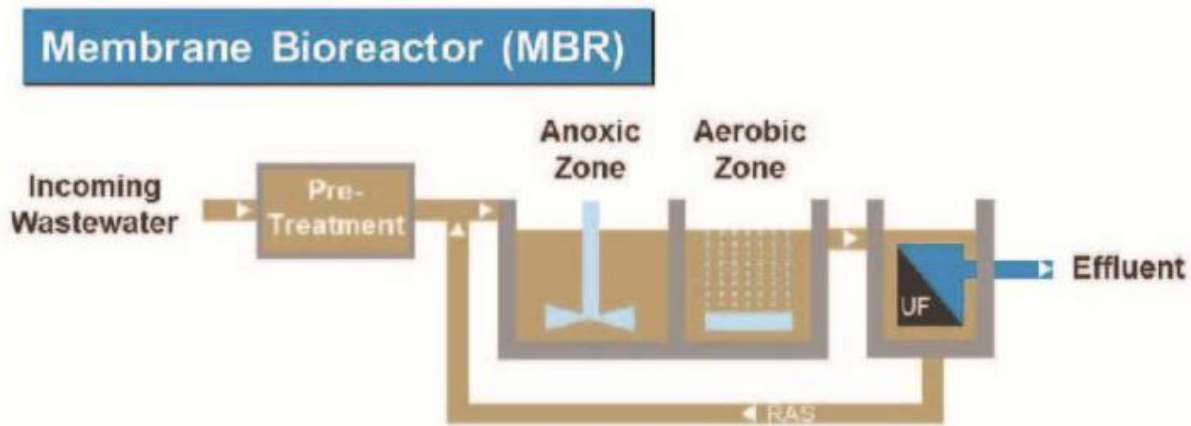


Figure 10-2 Diagram of a traditional membrane bioreactor (MBR) layout showing how pre-treatment is implemented to help reduce membrane fouling¹

10.3. Other Coatings and Coating Techniques

A total of 5 different coatings were tested in this project: glycerol, dish detergent, and 3 different molecular weights of PVP. However, there are numerous other coatings that fit the criteria listed in section 8.3, which may cause the xylem to rewet better than the PVP. Based on the results for the preservation testing, it appears that the polymer must be smaller than the cutoff diameter for it to penetrate the pores and effectively coat the sample. Otherwise, it appears that the coating is just filtered out like any other retentate. So, for white pine, we have an additional criteria that the size must be smaller than 100 nm. Other coating methods should be considered as well, beyond

the ones spelled out in this paper. It may be more effective to soak the xylem in a solution bath of PVP before letting them dry to allow more of the polymers to penetrate the membranes.

10.4. Virus Filtration

A major requirement for plant xylem to be an effective solution to the world's potable water demand is its ability to reject viruses from the feed solution. As mentioned above, the effective cutoff length for particle filtration using *pinus strobus* is roughly 100 nm, while viruses are on the order of 20-100 nm. However, the pore size of xylem varies significantly across different species, with some having pores on the order of 10 nm. As a result, these species may be able to filter viruses without any modification.

Alternatively, just as the xylem was modified using the PVP coatings to prevent drying, other coatings may be able to partially block some of the pores and reduce their effective size. This would allow the xylem to reject particles smaller than 100 nm. We also observed in section 4.4 that the rejection rate of the xylem increased as a function of fouling from the retentate. Therefore, if we want xylem to reject viruses, a pre-treatment solution may be flushed through the xylem with particles designed specifically to foul the xylem.

10.5. Preparation & Packaging

Once the top performing species of plant is identified, distribution of the xylem will need to be considered. During the duration of this thesis, branches could still function as effective filters several weeks after being cut from a tree so long as they were kept in water. Additionally, the PVP coatings tested in this paper showed that the xylem are able to rewet to a percentage of their initial permeability; however, to meet the global demand for drinking water, a large volume of samples will be required because they have a limited life due to fouling. This means that the trees will either need to be grown locally and harvested as needed, or packaged and shipped to their final destination regularly.

The diameter of the sample must correspond to the inner diameter of the hosing used. Larger branches can be cut down to the proper diameter, but in doing so their cylindrical shape must be preserved, otherwise the hosing may not form a tight seal around the perimeter of the xylem and feed solution may leak through. A more reliable technique than using an industrial razor should be developed for performing this task.

Finally, the clamping force used on the hose clamp has an effect on the performance of the xylem. Too little force will allow water to leak past, while too much can crush the xylem and either reduce permeability or even entirely prevent flow through it. Tests should be done to determine the optimal clamping force and a reliable way of repeatedly achieving that value should be developed.

10.6. Removing Fouled Portion

As we saw with the 300x diluted red ink in section 305.3, the bulk of the ink particles filtered by the xylem were removed from the feed solution within the first 0.1in of the sample. From the fouling tests in section 7.3, we saw that the permeability dropped off dramatically as filtered ink particles began to clog the xylem pores. If only the top portion of the sample is fouling and the majority of it isn't effected, than removing the fouled portion may return the xylem's permeability to a higher percentage of its initial value. This way, if the end user can begin with a longer sample than needed and simply remove small lengths of the xylem as it fouls. This would allow them to use the same sample for multiple filtrations, reducing the total number of samples required.

10.7. Implementation

Many attempts have been made at making potable water available at a low cost to the masses in developing countries using various technologies. One of the key issues all of these solutions face, including using plant xylem, is gaining traction. As with any innovation, there will be social challenges associated with adoption of a new technology. For the end user, water is most likely something that is free or already very inexpensive for them. So, convincing them that they should take these extra steps and incur additional costs to purify water, which they may not believe is fouled, may be a challenge. The best way of accomplishing this will be to have boots on the ground, either working with villages one at a time, or working with government officials to instigate clean water education programs.

Bibliography

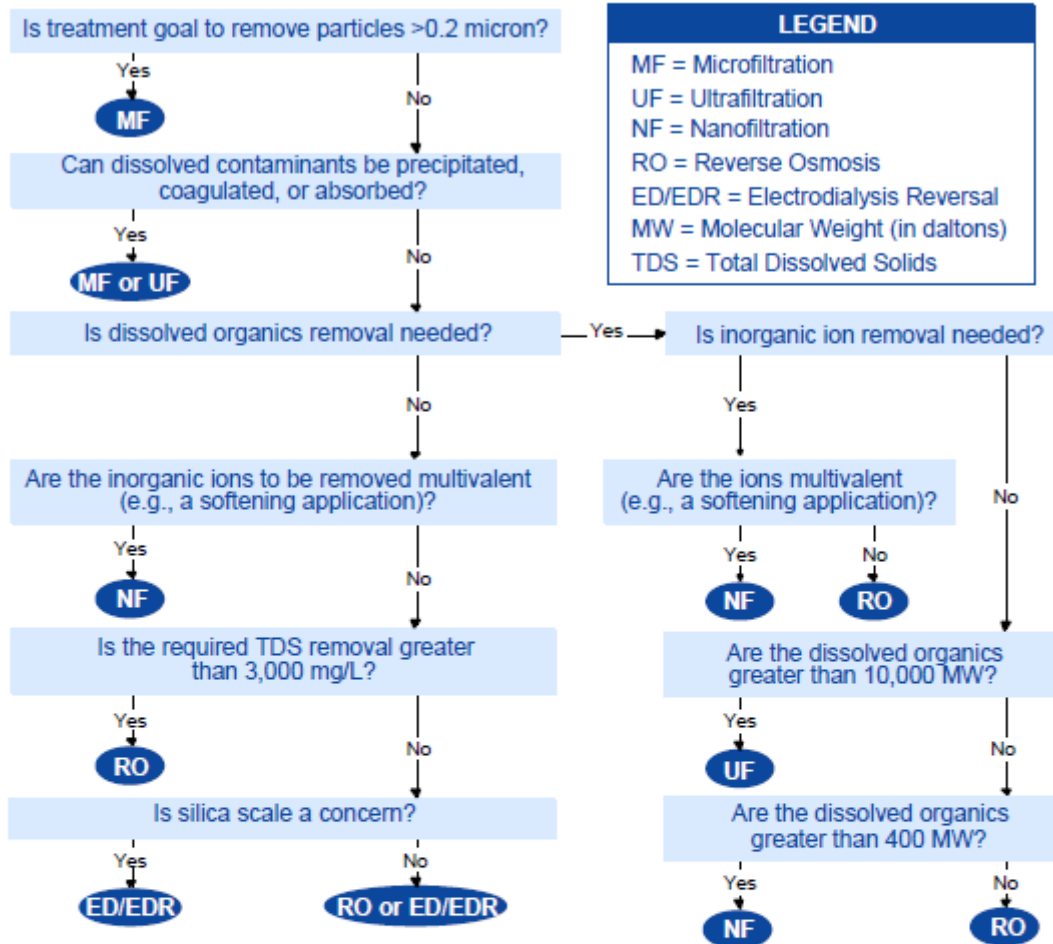
- [1] A Koch Chemical Technology Group, LLC Company. (2013). *Membrane Filtration Technology: Meeting Today's Water Treatment Challenges*.
- [2] Bouchard, C., Carreau, P., Matsuura, T., & Sourirajan, S. (1994). Modeling of ultrafiltration: Predictions of Concentration Polarization Effects. *Journal of Membrane Science*, 215-229.
- [3] Burdett, J. K. (1995). *Chemical Bonding in Solids*. New York: Oxford University Press.
- [4] Center for Disease Control and Prevention. (2014, 5 2). *Parasites - Ascariasis*. Retrieved from http://www.cdc.gov/parasites/ascariasis/gen_info/faqs.html
- [5] *Chlamydia trachomatis*. (2014, 5 2). Retrieved from MicrobeWiki: http://microbewiki.kenyon.edu/index.php/Chlamydia_trachomatis
- [6] Choat, B., Ball, M., Luly, J., & Holtum, J. (2003). Pit membrane porosity and water stress-induced cavitation in four co-existing dry rainforest tree species. *Plant Physiol*, 41-48.
- [7] Choat, B., Cobb, A. R., & Jansen, S. (2008). Structure and function of bordered pits: new discoveries and impacts on whole-plant hydraulic function. *New Phytol*, 608-625.
- [8] De Zuane, J. (1997). *Handbook of Drinking Water Quality*. New York: Van Nostrand 575 pp. 2nd ed.
- [9] Fenwick, A. (Mar, 2012). The Global Burden of Neglected Tropical Diseases. *Public Health*, pp. 126 (3): 233-6.
- [10] Gadgil, A. (1998, November). Drinking Water in Developing Countries. *Annual Review of Energy and the Environment*, p. 253.
- [11] Grenier, A., Meireles, M., Aimar, P., & Carvin, P. (2008). Analysing Flux Decline in Dead-End Filtration. *Chemical Engineering Research and Design*, 1281-1293.
- [12] Hughey, D. B. (2014, April 8). *CASE 1 Statistical Method*. Retrieved from 2.671 Measurement and Instrumentation: <https://wikis.mit.edu/confluence/display/2DOT671/CASE+1+Statistical+Method>
- [13] Hughey, D. B. (2014, April 4). *t-factor table*. Retrieved from 2.671 Measurement and Instrumentation: <https://wikis.mit.edu/confluence/display/2DOT671/t-factor+table>

- [14] Jansen, S., Choat, B., & Pletsers, A. (2009). Morphological Variation of Intervessel Pit Membranes and Implications to Xylem Function in Angiosperms. *Am J Bot*, 409-419.
- [15] Khalil G. Ghanem, M., & Trevor A. Crowell, M. (2014, 5 2). *Hookworm*. Retrieved from Johns Hopkins Antibiotic (ABX) Guide: http://www.hopkinsguides.com/hopkins/ub/view/Johns_Hopkins_ABX_Guide/540275/all/Hookworm
- [16] Lee, J., Boutillier, M. H., Chambers, V., & Karnik, R. (2014). Water Filtration Using Plant Xylem. 1-11.
- [17] Loo, S. L., Fane, A. G., Krantz, W. B., & Lim, T. T. (2012). Emergency water supply: A review of potential technologies and selection criteria. *Water Research*, 3125-3151.
- [18] Madaeni, S. S. (1999). The application of membrane technology for water disinfection. *Water Research*, 301-308.
- [19] National Environmental Services Center. (1999). Membrane Filtration. *Tech Brief*, pp. 2, 7. Retrieved from http://www.nesc.wvu.edu/pdf/dw/publications/ontap/2009_tb/membrane_DWFSOM43.pdf
- [20] Petty, J. (1972). Aspiration of Bordered Pits in Conifer Wood. *Proc R Soc Ser B-Bio*, 395-406.
- [21] Poirier, M. R. (2014, 5 2). *Filtration Systems, Inc., Report for WSRC SpinTek Rotary Microfilter Testing*. Retrieved from Filtration Systems, Inc., Report for WSRC SpinTek Rotary Microfilter Testing
- [22] Sandy Cairncross, R. M. (2002). Dracunculiasis (Guinea Worm Disease) and the Eradication Initiative. *Clinical Microbiology Reviews*, 223-246.
- [23] *Seal Face Lubrication*. (2014, 5 2). Retrieved from Mc Nally Institute: <http://www.mcnallyinstitute.com/09-html/09-07.html>
- [24] Sperry, J. (2003). Evolution of water transport and xylem structure. *Int J Plant Sci*, S115-S127.
- [25] Stanford University. (2014, 5 2). *Ascariasis*. Retrieved from ParaSite: http://www.stanford.edu/group/parasites/ParaSites2005/Ascaris/JLora_ParaSite.htm
- [26] Thétiot-Laurent, S., Boissier, J., Robert, A., & Meunier, B. (2013, Jun 27). Schistosomiasis Chemotherapy. *Angewandte Chemie (International ed. in English)*, pp. 52 (31): 7936–56.

- [27] United States Department of Agriculture. (2014, 5 2). *Pinus strobus L. Eastern white pine*. Retrieved from Natural Resources Conservation Service: <https://plants.usda.gov/core/profile?symbol=PIST>
- [28] University of Cambridge Schistosomiasis Research Group. (2014, 5 2). *Life Cycle of Schistosoma mansoni - The Egg*. Retrieved from http://www.path.cam.ac.uk/~schisto/schistosoma/schisto_lifecycle_egg.html
- [29] World Health Organization. (1993-1998). *Guidelines for Drinking Water Quality*. Vols. 1-3. Geneva, Switz: WHO.
- [30] World Health Organization. (2014, 5 2). *10 facts on guinea-worm disease*. Retrieved from http://www.who.int/features/factfiles/guinea_worm/en/
- [31] World Health Organization. (2014, 5 2). *Diarrhoeal disease*. Retrieved from <http://www.who.int/mediacentre/factsheets/fs330/en/>
- [32] World Health Organization. (2014, 5 2). *Dracunculiasis (guinea-worm disease)*. Retrieved from <http://www.who.int/mediacentre/factsheets/fs359/en/>
- [33] World Health Organization. (2014, 5 2). *Trachoma*. Retrieved from <http://www.who.int/blindness/causes/trachoma/en/>
- [34] World Health Organization. (2014, 5 2). *Water Sanitation Fact Sheet N112*. Retrieved from <http://www.who.int/inf-fs/en/fact112.html>

Appendix A: Additional References on Filtration¹

Figure 1: Generalized Membrane Process Selection Chart



LEGEND	
MF	= Microfiltration
UF	= Ultrafiltration
NF	= Nanofiltration
RO	= Reverse Osmosis
ED/EDR	= Electrodialysis Reversal
MW	= Molecular Weight (in daltons)
TDS	= Total Dissolved Solids

NOTE: This simplified chart is based on common assumptions and should not be applied to every situation without more detailed analysis.

ASSUMPTIONS	
<p>A. Relative Cost</p> <ul style="list-style-type: none"> MF < UF < NF < RO or ED/EDR If TDS removal > 3,000 mg/L, RO or ED/EDR may be less costly 	<p>B. Removals</p> <ul style="list-style-type: none"> MF—particles > 0.2 Micron UF—organics > 10,000 MW, virus, and colloids NF—organics > 400 MW and hardness ions RO—salts and low MW organics ED/EDR—Salts Particles include <i>Giardia</i>, <i>Cryptosporidium</i>, bacteria, and turbidity

Reprinted from Proceedings of the 1993 Membrane Technology Conference, by permission. Copyright ©1993, American Water Works Association.

Figure 10-1 Flow chart used for determining the optimal filtration method based on feed solution¹

Appendix B: Uncertainty Analysis Resources¹¹

$\nu = n - m$ where n is the number of measurements and m is the number of adjustable parameters

Table 8 – t -factor table used for uncertainty analysis¹²

ν	t_ν	ν	t_ν	ν	t_ν
1	12.706	11	2.201	21	2.080
2	4.303	12	2.179	22	2.074
3	3.182	13	2.160	23	2.069
4	2.776	14	2.145	24	2.064
5	2.571	15	2.131	25	2.060
6	2.447	16	2.120	26	2.056
7	2.365	17	2.110	27	2.052
8	2.306	18	2.101	28	2.048
9	2.262	19	2.093	29	2.045
10	2.228	20	2.086	30	2.042

$$\bar{x} = \frac{\sum x_i}{N}$$
$$\sigma_x = \sqrt{\frac{\sum (x_i - \bar{x})^2}{N - 1}}$$
$$u_x = \frac{t_\nu \sigma_x}{\sqrt{N}}$$

For values of $\nu > 30$ use $t_\nu = 2.0$. The 95% confidence interval is then $\bar{x} \pm u_x$